

European Journal of Applied Mathematics

<http://journals.cambridge.org/EJM>

Additional services for *European Journal of Applied Mathematics*:

Email alerts: [Click here](#)

Subscriptions: [Click here](#)

Commercial reprints: [Click here](#)

Terms of use : [Click here](#)



High-frequency spectral analysis of thin periodic acoustic strips: Theory and numerics

S. D. M. ADAMS, K. D. CHEREDNICHENKO, R. V. CRASTER and S. GUENNEAU

European Journal of Applied Mathematics / Volume 21 / Issue 06 / December 2010, pp 557 - 590
DOI: 10.1017/S0956792510000215, Published online: 27 July 2010

Link to this article: http://journals.cambridge.org/abstract_S0956792510000215

How to cite this article:

S. D. M. ADAMS, K. D. CHEREDNICHENKO, R. V. CRASTER and S. GUENNEAU (2010). High-frequency spectral analysis of thin periodic acoustic strips: Theory and numerics. European Journal of Applied Mathematics, 21, pp 557-590 doi:10.1017/S0956792510000215

Request Permissions : [Click here](#)

High-frequency spectral analysis of thin periodic acoustic strips: Theory and numerics

S. D. M. ADAMS¹, K. D. CHEREDNICHENKO², R. V. CRASTER³
and S. GUENNEAU⁴

¹*Department of Mathematics, Imperial College London, London SW7 2AZ, UK*

²*School of Mathematics, Cardiff University, Senghennydd Road, Cardiff CF24 4AG, UK*

³*Department of Mathematical and Statistical Sciences, University of Alberta, Edmonton, Canada T6G 2G1
email: craster@ualberta.ca*

⁴*Department of Mathematical Sciences, Liverpool University, Liverpool L69 3BX, UK*

(Received 27 May 2009; revised 22 June 2010 and accepted 24 June 2010;
first published online 27 July 2010)

This paper is devoted to the study of the asymptotic behaviour of the high-frequency spectrum of the wave equation with periodic coefficients in a ‘thin’ elastic strip $\Sigma_\eta = (0, 1) \times (-\eta/2, \eta/2)$, $\eta > 0$. The main geometric assumption is that the structure period is of the order of magnitude of the strip thickness η and is chosen in such a way that η^{-1} is a positive large integer. On the boundary $\partial\Sigma_\eta$, we set Dirichlet (clamped) or Neumann (traction-free) boundary conditions. Aiming to describe sequences of eigenvalues of order η^{-2} in the above problem, which correspond to oscillations of high frequencies of order η^{-1} , we study an appropriately rescaled limit of the spectrum. Using a suitable notion of two-scale convergence for bounded operators acting on two-scale spaces, we show that the limiting spectrum consists of two parts: the Bloch (or band) spectrum and the ‘boundary’ spectrum. The latter corresponds to sequences of eigenvectors concentrating on the vertical boundaries of Σ_η , and is characterised by a problem set in a semi-infinite periodic strip with either clamped or stress-free boundary conditions. Based on the observation that some of the related eigenvalues can be found by solving an appropriate periodic-cell problem, we use modal methods to investigate finite-thickness semi-infinite waveguides. We compare our results with those for finite-thickness infinite waveguides given in Adams *et al.* (*Proc. R. Soc. Lond. A*, vol. 464, 2008, pp. 2669–2692). We also study infinite-thickness semi-infinite waveguides in order to gain insight into the finite-height analogue. We develop an asymptotic algorithm making use of the unimodular property of the modal method to demonstrate that in the weak contrast limit, and when wavenumber across the guide is fixed, there is at most one surface wave per gap in the spectrum. Using the monomode property of the waveguide we can consider the gap structure for the n th mode, when doing so, for traction-free boundaries, we find exactly one surface wave in each n -band gap.

1 Introduction

We are concerned with the asymptotic analysis of a sequence of spectral problems for the acoustic wave equation displaying rapidly oscillating coefficients of period η within a strip $\Sigma_\eta = (0, 1) \times (-\eta/2, \eta/2)$, where $\eta > 0$ is such that η^{-1} is a large positive integer.

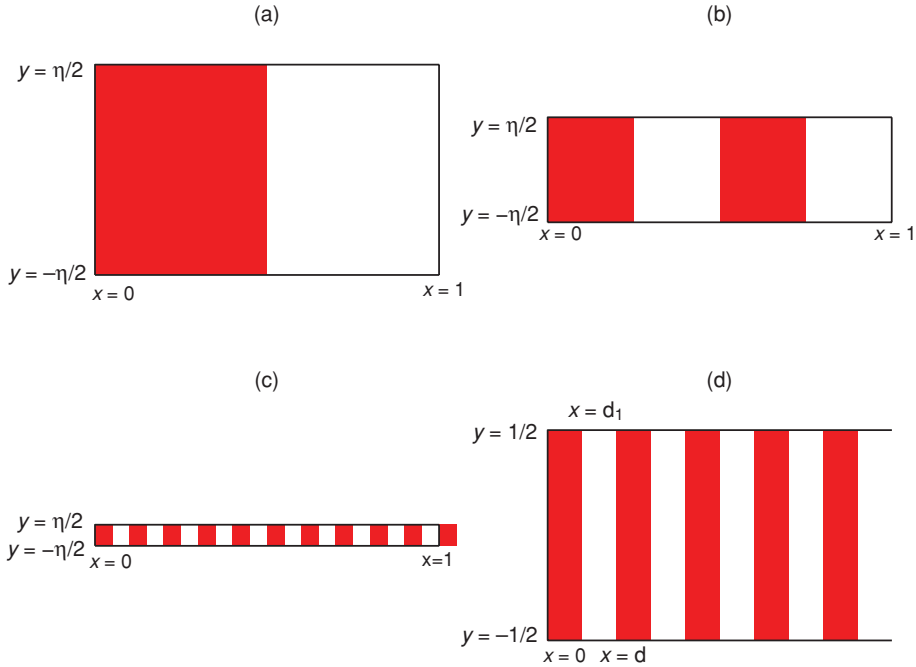


FIGURE 1. (Colour online) A sketch of the strip geometry we consider in the analysis, for clarity shown here with piecewise constant parameters to give a layered medium. (a)–(c) The problem as $\eta = N^{-1} \rightarrow 0$ as considered in the analysis of Section 2. (a) $N = 1$, (b) $N = 2$ and (c) $N = 10$. (d) The semi-infinite strip geometry, which we consider in the numerical results of Section 3. The coordinates (x, y) are equivalent to (x_1, x_2) .

Figures 1(a)–(c) show how a guide with piecewise constant material parameters changes in the limit as $\eta \rightarrow 0$. The partial differential equation we consider is supplied with either homogeneous Dirichlet or Neumann boundary conditions on the boundary $\partial\Sigma_\eta$. This kind of problem models the acoustic vibrations of a periodic strip with clamped and/or traction-free boundaries, and is of current interest for the physics community since it has potential applications in acousto-optic polarizers, slow elastic waves and high-resolution endoscopes (Pagneux & Maurel, 2002; Russell *et al.*, 2003; Adams *et al.*, 2008, 2009).

The interest in periodic structures has recently shifted from the analysis of their band structure (Pendry, 1994) (well described in the one-dimensional setting by a Kronig–Penney model, Kronig & Penney, 1931) to anomalous dispersion (e.g. very high dispersion, Lin *et al.*, 1996; vanishing dispersion, i.e. slow light, Figotin & Vitebskiy, 2006; or negative group velocity associated with negative refraction Gralak *et al.*, 2000) and defect states (forming the foundation of cavities with unprecedented quality factors).

It is known in solid-state physics that for high curvature bands (i.e. small effective mass), defect levels tend to remain close to the band edge: e.g. a shallow defect in a semiconductor can be described by a hydrogen atom model (Kohn & Luttinger, 1955) in which the ionization energy, which is the energy of the defect’s ground state, is proportional to the effective mass. This has recently drawn attention to the band-edge properties of

periodic structures (Dossou *et al.*, 2007), where manipulation of the dispersion curves very close to a band gap edge can lead to extremely low group velocity over extended frequency ranges (Figotin & Vitebskiy, 2006).

We assume that the frequency is high enough to warrant the existence of scale interaction effects between the wavelength and the microscopic length scale of the medium. Several works investigating this possibility using spectral asymptotic tools have been written by Allaire and Conca, in the context of fluid–solid structures (Allaire & Conca, 1996, 1998a), as well as for a scalar elliptic equation with Dirichlet boundary conditions (Allaire & Conca, 1998b). Castro and Zuazua further investigated the asymptotic spectrum of a clamped string with rapidly oscillating density, which displays stop bands and boundary modes associated with concentration effects at the string ends (Castro and Zuazua, 1996; Castro & Zuazua, 2000a, 2000b). Similar effects arise in multi-layered elastic (Camley *et al.*, 1983) and dielectric (Zolla *et al.*, 2008) structures, in slow-diffusion problems for highly heterogeneous media with an interface (Allaire & Capdeboscq, 2002) and in vibrating systems with many concentrated masses (Lobo & Pérez, 2001 and references therein).

Whereas two of us previously used the tools developed by Allaire and Conca to look at similar problems arising in the context of infinite three-dimensional photonic crystals (Cherednichenko & Guenneau, 2007), where no concentration effects occur, our present paper deals with a strip problem in the context of acoustic waves: the specific geometry (periodic in one direction, finite in the other) requires an analysis of its own.

Some notational conventions that we adopt throughout the text have to be mentioned. We think of any two functions u and v that take different values on a set of Lebesgue measure zero as being the same, and write $u = v$. Also, in all formulae u_i denotes partial differentiation with respect to the variable x_i , $i = 1, 2$. Finally, \mathbf{x} everywhere stands for (x_1, x_2) .

We analyse the propagation of transverse acoustic modes in a thin strip with clamped or traction-free top and bottom walls, as shown in Figure 1. The typical heterogeneity size along the waveguide (the thickness of the layers) is characterised by a small positive parameter η and the shear modulus μ_η and density ρ_η are assumed to be of the form $\mu_\eta = \mu(x_1/\eta, x_2/\eta)$, $\rho_\eta = \rho(x_1/\eta, x_2/\eta)$, where $\mu(x'_1, x'_2)$, $\rho(x'_1, x'_2)$ are measurable real-valued functions that are 1-periodic in the variable x'_i and such that $0 < c_1 \leq \mu, \rho \leq c_2 < \infty$ almost everywhere for some constants c_1, c_2 . Throughout our work we assume that η^{-1} is an integer. The task of finding the *modes* in such a structure amounts to looking for pairs $(\lambda_\eta, u_\eta) \in \mathbb{C} \times H^1(\Sigma_\eta)$ with $u_\eta \neq 0$ that satisfy the following eigenvalue problem:

$$-\rho^{-1}(\mathbf{x}/\eta) \nabla \cdot (\mu(\mathbf{x}/\eta) \nabla u_\eta(\mathbf{x})) = \lambda_\eta u_\eta(\mathbf{x}), \quad \mathbf{x} \in \Sigma_\eta, \quad (1.1)$$

$$u_\eta|_{x_1=0} = u_\eta|_{x_1=1} = 0 \quad \text{or} \quad (u_\eta)_{,x_1}|_{x_1=0} = (u_\eta)_{,x_1}|_{x_1=1} = 0, \quad x_2 \in (-\eta/2, \eta/2), \quad (1.2)$$

$$u_\eta|_{x_2=-\eta/2} = u_\eta|_{x_2=\eta/2} = 0 \quad \text{or} \quad (u_\eta)_{,x_2}|_{x_2=-\eta/2} = (u_\eta)_{,x_2}|_{x_2=\eta/2} = 0, \quad x_1 \in (0, 1). \quad (1.3)$$

The first pair of conditions in (1.2) (respectively, (1.3)) corresponds physically to the case of clamped boundaries at $x_1 = 0, 1$ (respectively, $x_2 = \pm\eta/2$), while the second pair models the case when these boundaries are free to vibrate.

The problem (1.1)–(1.3) is understood in the weak sense, as follows. Denote by \mathcal{H}_η the closure in $H^1(\Sigma_\eta)$ of the set of infinitely smooth functions on $\bar{\Sigma}_\eta$ that vanish on those

parts of the boundary $\partial\Sigma_\eta$ that are clamped, and the set $H^1(\Sigma_\eta)$ itself in the case when the whole of $\partial\Sigma_\eta$ is free to vibrate (which corresponds to the second pair of conditions in (1.2) and (1.3)). Then we say that (1.1)–(1.3) holds if $u_\eta \in \mathcal{H}_\eta$ and the integral identity

$$\int_{\Sigma_\eta} \mu(x_1/\eta, x_2/\eta) \nabla u(\mathbf{x}) \cdot \nabla \varphi(\mathbf{x}) d\mathbf{x} = \int_{\Sigma_\eta} \rho(x_1/\eta, x_2/\eta) f(\mathbf{x}) \varphi(\mathbf{x}) d\mathbf{x} \tag{1.4}$$

holds with $u = u_\eta$ and $f = \lambda_\eta u_\eta$, for any $\varphi \in \mathcal{H}_\eta$. One can define an operator \mathcal{A}_η on a dense subset of $L^2(\Sigma_\eta)$, such that (1.4) is equivalent¹ to $\mathcal{A}_\eta u = f$ for any $f \in L^2(\Sigma_\eta)$. Clearly, for each η the operator \mathcal{A}_η is self-adjoint and non-negative, so that the set of λ_η in (1.1)–(1.3) is in fact a subset of $[0, +\infty)$. It is also known that for each $\eta > 0$ the operator \mathcal{A}_η has compact resolvent, and therefore its spectrum σ_η is a sequence $\{\lambda_\eta^j\}_{j=1}^\infty$ of discrete eigenvalues with $+\infty$ as the only accumulation point. For every eigenvalue λ_η^j there corresponds an eigenfunction $v_\eta^j \in L^2(\Sigma_\eta)$ such that $\|v_\eta^j\|_{L^2(\Sigma_\eta)} = 1$, and the family v_η^j is an orthonormal basis in $L^2(\Sigma_\eta)$ (see e.g. Bensoussan et al., 1978).

A natural problem is to determine the asymptotic behaviour of σ_η when the period η tends to zero. In this paper we study the case when the wavelength remains in resonance with the period/thickness η during the limiting process, i.e. we are looking for the high-frequency regime within which so-called band gaps and localised modes may occur as in Castro & Zuazua (2000b), Conca et al. (1995) and Figotin & Kuchment (1996). To be more precise, we wish to study the asymptotic behaviour of the set $\eta^2 \sigma_\eta$ as $\eta \rightarrow 0$. In what follows we pay special attention to both the analytical and numerical characterisation of modes, whose support concentrates in the neighbourhood of the waveguide vertical boundaries $x_1 = 0, 1$.

2 The two-scale analysis of (1.1)–(1.3)

In this section we focus on the second, Neumann-type, case of boundary conditions in (1.2) and (1.3). The analysis of the problems with Dirichlet-type conditions on some of the four sides of $\partial\Sigma_\eta$ is completely analogous and so, for brevity, is omitted. In order to obtain the necessary *a priori* estimates and then use appropriate compactness principles, we choose to study the operator $\mathcal{A}_\eta + \eta^{-2}\mathcal{I}$ rather than \mathcal{A}_η , which obviously shifts the spectrum of (1.1)–(1.3) through η^{-2} in the positive direction.

We denote $N := \eta^{-1}$, recalling that $N \in \mathbb{N}$, and make the rescalings $\mathbf{x}' = \mathbf{x}/\eta \equiv N(x_1, x_2)$ $\lambda_\eta = \eta^{-2}\lambda \equiv N^2\lambda$ in the equation obtained at the previous step, which leads to

¹ More precisely, define a quadratic form $[\cdot, \cdot]$ on \mathcal{H}_η by the formula $[u, u] = \int_{\Sigma_\eta} \mu(x_1/\eta, x_2/\eta) \nabla u(\mathbf{x}) \cdot \nabla u(\mathbf{x}) d\mathbf{x}$. For each $f \in L^2(\Sigma_\eta)$ the expression $F_f(\varphi) := \int_{\Sigma_\eta} \rho(x_1/\eta, x_2/\eta) f(\mathbf{x}) \varphi(\mathbf{x}) d\mathbf{x}$ is a linear functional on \mathcal{H}_η , which is continuous with respect to the norm $\sqrt{[u, u]}$. Hence, by the Riesz theorem, there exists an element $u_\eta(f) \in \mathcal{H}_\eta$ such that $[u_\eta(f), \varphi] = F_f(\varphi)$ for any $\varphi \in \mathcal{H}_\eta$. Note that if $f \neq 0$ then $u_\eta(f) \neq 0$. Indeed, if $u_\eta(f) = 0$ then for a sequence $\varphi_n \in \mathcal{H}_\eta$ that converges in $L^2(\Sigma_\eta)$ to f we have $0 = [u_\eta(f), \varphi_n] = \int_{\Sigma_\eta} f \varphi_n \rightarrow \|f\|_{L^2(\Sigma_\eta)}^2$ as $n \rightarrow \infty$, hence $f = 0$. The operator \mathcal{A}_η is now defined on the set $\{u_\eta(f) : f \in L^2(\Sigma_\eta)\}$ by the formula $\mathcal{A}_\eta u_\eta(f) = f$.

the spectral problem

$$-\rho^{-1}(\mathbf{x})\nabla \cdot (\mu(\mathbf{x})\nabla u(\mathbf{x})) + u(\mathbf{x}) = \lambda u(\mathbf{x}), \quad \mathbf{x} := (x_1, x_2) \in \Omega_N := (0, N) \times (-1/2, 1/2), \quad (2.1)$$

$$u_{,1}|_{x_1=0} = u_{,1}|_{x_1=N} = 0, \quad u_{,2}|_{x_2=-1/2} = u_{,2}|_{x_2=1/2} = 0, \quad (2.2)$$

where for convenience we write \mathbf{x} instead of \mathbf{x}' . As in the case of (1.1)–(1.3), the problem (2.1)–(2.2) is understood in the weak sense, i.e. $u \in H^1(\Omega_N)$ and for any $\varphi \in H^1(\Omega_N)$ one has

$$\int_{\Omega_N} \mu \nabla u \cdot \nabla \varphi + \int_{\Omega_N} \rho u \varphi = \lambda \int_{\Omega_N} \rho u \varphi. \quad (2.3)$$

Denote by σ_N the set of eigenvalues λ in the problem (2.1)–(2.2).

In the rest of Section 2 we describe the limiting behaviour of the spectra σ_N as $N \rightarrow \infty$. In particular, we show that the appropriately defined limit of σ_N as $N \rightarrow \infty$ consists of elements of two types (which are not necessarily disjoint), namely those that we refer to as the boundary spectrum and the standard Bloch spectrum of the related problem in the strip $\mathbb{R} \times (-1/2, 1/2)$. This is the subject of Section 2.2, following the definition of the boundary spectrum in Section 2.1. Further, in Section 2.3 we show that the boundary spectrum, like the Bloch spectrum, is contained in the spectrum σ_{Π} of an appropriate problem on the semi-infinite strip $(0, +\infty) \times (-1/2, 1/2)$. Finally, in Sections 2.4 and 2.5, using the concept of a ‘boundary two-scale convergence’ for sequences of functions on Ω_N , we establish the fact that σ_{Π} is contained in the limit of the spectra σ_N as $N \rightarrow \infty$. The argument of Section 2 as a whole thus aims at a ‘sandwich-type’ formula (2.26), which provides the basis for identifying, in Section 3, eigensequences of the ‘boundary-type’.

2.1 Boundary spectrum

We begin with a definition of the boundary spectrum.

Definition 1 *We shall say that λ is an element of the boundary spectrum if there exists a sequence of normalised ($\|u_N\|_{L^2(\Omega_N)} = 1$) eigenfunctions u_N for the problems (2.1)–(2.2), $N \in \mathbb{N}$, whose eigenvalues λ_N converge to λ as $N \rightarrow \infty$, and such that for any sequence $\{a_N\}_{N=1}^{\infty}$, $a_N > 0$, $N \in \mathbb{N}$, satisfying $a_N/N \rightarrow 0$ as $N \rightarrow \infty$ one has $\|u_N\|_{L^2(\omega_N)} \rightarrow 0$ as $N \rightarrow \infty$, where $\omega_N := (N/2 - a_N/2, N/2 + a_N/2) \times (-1/2, 1/2)$.*

Remark 1 It is clear that without loss of generality one can consider in the above definition only those sequences a_N for which $a_N < N/4$, $N \in \mathbb{N}$, and $a_N \rightarrow \infty$ as $N \rightarrow \infty$, with other requirements of the definition preserved.

Let us denote by σ_{boundary} the set of all possible values λ in the definition above. Henceforth we also use the notation $I_1 := (0, 1)$, $I_2 := (-1/2, 1/2)$, $\mathbb{R}_+ := (0, +\infty)$, $\Pi := \mathbb{R}_+ \times I_2$.

For each $\theta \in [0, 1)$ consider the eigenvalue problem

$$-\rho^{-1}(\mathbf{x})(\nabla + 2\pi\theta\mathbf{e}_1) \cdot (\mu(\mathbf{x})(\nabla + 2\pi\theta\mathbf{e}_1)u(\mathbf{x})) + u(\mathbf{x}) = \lambda(\theta)u(\mathbf{x}), \quad \mathbf{x} \in I_1 \times I_2, \quad (2.4)$$

$$u|_{x_1=0} = u|_{x_1=1}, \quad u_{,1}|_{x_1=0} = u_{,1}|_{x_1=1}, \quad u_{,2}|_{x_2=-1/2} = u_{,2}|_{x_2=1/2} = 0, \quad (2.5)$$

where $\mathbf{e}_1 = (1, 0)$.

We define an operator S on $L^2(\Pi)$ by the formula $Sf = u$, where for each $f \in L^2(\Pi)$ the function $u \in H^1(\Pi)$ is such that (cf. (2.3))

$$\int_{\Pi} \mu \nabla u \cdot \nabla \varphi + \int_{\Pi} \rho u \varphi = \int_{\Pi} \rho f \varphi \quad (2.6)$$

for any $\varphi \in H^1(\Pi)$. It is well known that the set σ_{Bloch} ('Bloch spectrum') consisting of the inverses $\lambda(\theta)^{-1}$ of all eigenvalues $\lambda(\theta)$ in (2.4)–(2.5) as $\theta \in [0, 1)$, is the continuous spectrum of the operator S (see e.g. Kuchment, 1993).

2.2 The structure of the limit spectrum

We next show that a 'completeness' result holds as $N \rightarrow \infty$, namely that the limiting values of λ as $N \rightarrow \infty$ in (2.1)–(2.2) are either of the 'Bloch-type', or of the 'boundary-type', or both. In the proof of the following theorem we follow the approach of Allaire & Conca (1998b) and Cherednichenko & Guenneau (2007).

Theorem 1 *If $\lambda \in \lim_{N \rightarrow \infty} \sigma_N$ and $\lambda \notin \sigma_{\text{boundary}}$, then $\lambda \in \sigma_{\text{Bloch}}$.*

Proof Suppose $\lambda \in \lim_{N \rightarrow \infty} \sigma_N \setminus \sigma_{\text{boundary}}$. Then there exists a sequence of eigenfunctions u_N of the problem (2.1)–(2.2), $\|u_N\|_{L^2(\Omega_N)} = 1$, with eigenvalues $\lambda_N \rightarrow \lambda$ as $N \rightarrow \infty$, and a sequence $\{a_N\}_{N=1}^{\infty}$, $a_N > 0$, $N \in \mathbb{N}$, such that $a_N \rightarrow \infty$, $a_N/N \rightarrow 0$ as $N \rightarrow \infty$, and $\|u_N\|_{L^2(\omega_N)} \geq c_3 > 0$ for any $N \in \mathbb{N}$.

Consider a sequence of smooth functions ψ_N in $(0, N)$ such that $\psi_N(x_1) = 1$ for $x_1 \in (N/2 - a_N/2, N/2 + a_N/2)$, $\psi_N(x_1) = 0$ for $x_1 \in (0, N/2 - a_N) \cup (N/2 + a_N, N)$ (recall that we can assume that $a_N < N/4$) and $|\psi'_N(x_1)| \leq 4/a_N$ for any $N \in \mathbb{N}$, $x_1 \in (0, N)$, where $\psi'_N(x_1) := d\psi_N/dx_1$; such sequences clearly exist. For the function

$$v_N(\mathbf{x}) = \|u_N(\mathbf{x})\psi_N(x_1)\|_{L^2(\Omega_N)}^{-1} u_N(\mathbf{x})\psi_N(x_1)$$

extended by zero to $\Pi \setminus \Omega_N$, one has $\|v_N\|_{L^2(\Pi)} = 1$, and the expression

$$R_N := -\rho^{-1} \nabla \cdot (\mu \nabla v_N) + v_N - \lambda_N v_N,$$

as an element of the dual space³ H^* to $H^1(\Pi)$, satisfies

$$\|w_N\|_{H^1(\Pi)}^{-1} \langle R_N, w_N \rangle \rightarrow 0 \quad (2.7)$$

² We say that σ_N converges to σ in the Hausdorff sense, and write $\sigma = \lim_{N \rightarrow \infty} \sigma_N$, if $\max\{\sup_{\lambda_1 \in \sigma_N} \inf_{\lambda_2 \in \sigma} |\lambda_1 - \lambda_2|, \sup_{\lambda_2 \in \sigma} \inf_{\lambda_1 \in \sigma_N} |\lambda_1 - \lambda_2|\} \rightarrow 0$ as $N \rightarrow \infty$.

³ The space of linear continuous functionals on $H^1(\Pi)$.

as $N \rightarrow \infty$ for any sequence $w_N \in H^1(\Pi)$, where $\langle \cdot, \cdot \rangle$ is the duality⁴ between H^* and $H^1(\Pi)$. Indeed, notice first that (2.3) with $u = \varphi = u_N$ yields

$$\|u_N\|_{H^1(\Omega_N)} \leq c_4 \|u_N\|_{L^2(\Omega_N)} = c_4 \quad (2.8)$$

for some $c_4 > 0$. Hence, using the Cauchy–Schwarz inequality,

$$\begin{aligned} |\langle R_N, w_N \rangle| &= \|u_N \psi_N\|_{L^2(\Omega_N)}^{-1} \left| \int_{\Omega_N} \mu (\nabla(u_N \psi_N) \cdot \nabla w_N - \nabla u_N \cdot \nabla(\psi_N w_N)) \right| \\ &= \|u_N \psi_N\|_{L^2(\Omega_N)}^{-1} \left| \int_{\Omega_N} \mu \psi'_N (u_N(w_N)_{,x_1} - w_N(u_N)_{,x_1}) \right| \\ &\leq \|u_N\|_{L^2(\omega_N)}^{-1} c_2 \max_{x_1 \in (0, N)} |\psi'_N(x_1)| \|u_N\|_{H^1(\Omega_N)} \|w_N\|_{H^1(\Pi)} \leq c_3^{-1} c_2 4 a_N^{-1} c_4 \|w_N\|_{H^1(\Pi)}. \end{aligned}$$

Notice next that there exists a unique family $\{v_N^j\}_{j=1}^N$ of functions in $H_{\text{per}}^1(I_1 \times I_2)$ (see Proposition 5 for a definition of $H_{\text{per}}^1(I_1 \times I_2)$) such that

$$v_N(\mathbf{x}) = \sum_{j=1}^N v_N^j(\mathbf{x}) \exp(2\pi i x_1 N^{-1} j), \quad \mathbf{x} \in \Omega_N, \quad (2.9)$$

where $i^2 = -1$. Indeed, a direct calculation shows that if (2.9) holds then

$$v_N^j(\mathbf{x}) = N^{-1} \sum_{m=1}^N v_N(x_1 + m, x_2) \exp(-2\pi i (x_1 + m) N^{-1} j), \quad \mathbf{x} \in \Omega_N, \quad (2.10)$$

where the function v_N is extended according to the rule $v_N(x_1 + N, x_2) = v_N(x_1, x_2)$, $\mathbf{x} \in \Omega_N$. Clearly, the functions v_N^j are 1-periodic in x_1 . Further, using an argument similar to that employed in deriving (2.10) one has

$$\|v_N\|_{L^2(\Omega_N)}^2 = N \sum_{j=1}^N \|v_N^j\|_{L^2(I_1 \times I_2)}^2. \quad (2.11)$$

Differentiating (2.10) yields $v_N^j \in H_{\text{per}}^1(I_1 \times I_2)$ and

$$\nabla v_N(\mathbf{x}) = \sum_{j=1}^N (\nabla + 2\pi i N^{-1} j \mathbf{e}_1) v_N^j(\mathbf{x}) \exp(2\pi i x_1 N^{-1} j), \quad \mathbf{x} \in \Omega_N,$$

which in particular implies (cf. (2.11))

$$\|\nabla v_N\|_{L^2(\Omega_N)}^2 = N \sum_{j=1}^N \|(\nabla + 2\pi i N^{-1} j \mathbf{e}_1) v_N^j\|_{L^2(I_1 \times I_2)}^2. \quad (2.12)$$

⁴ For $v \in L^2(\Pi)$, we think of it as an element of the space H^* acting according to the rule $\langle v, \varphi \rangle = \int_{\Pi} \rho v \varphi$ for any $\varphi \in H^1(\Pi)$. Likewise, for $V \in [L^2(\Pi)]^2$, $\varphi \in H^1(\Pi)$, we set $\langle \rho^{-1} \nabla \cdot V, \varphi \rangle = \int_{\Pi} V \cdot \nabla \varphi$.

Further, each of the functions v_N^j in the above family is a linear combination of the ‘Bloch eigenfunctions’ $V^k = V^k(\theta, \mathbf{x})$, $\theta \in (0, 1]$:

$$v_N^j(\mathbf{x}) = \sum_{k=1}^{\infty} \alpha_N^{jk} V^k(j/N, \mathbf{x}),$$

with some $\alpha_N^{jk} \in \mathbb{C}$. The functions V^k are normalised ($\|V^k(\theta, \cdot)\|_{L^2(I_1 \times I_2)} = 1$) solutions of (2.4) that correspond to some eigenvalues $\lambda(\theta) = \lambda^k(\theta)$. Note that by the Plancherel theorem $\|v_N^j\|_{L^2(I_1 \times I_2)}^2 = \sum_{k=1}^{\infty} |\alpha_N^{jk}|^2$ for each $j = 1, 2, \dots, N$, and so $1 = \|v_N\|_{L^2(\Omega_N)}^2 = N \sum_{j=1}^N \sum_{k=1}^{\infty} |\alpha_N^{jk}|^2$.

For each $N \in \mathbb{N}$ and a set of continuous, 1-periodic in θ and uniformly bounded functions $h^k = h^k(\theta)$, $k \in \mathbb{N}$, consider the ‘modulation’ of v_N (cf. Allaire & Conca, 1998b) defined by

$$\mathcal{M}[v_N](\mathbf{x}) = \sum_{j=1}^N \sum_{k=1}^{\infty} h^k(j/N) \alpha_N^{kj} V^k(j/N, \mathbf{x}) \exp(2\pi i x_1 N^{-1} j).$$

The definition of the remainder term R_N implies

$$\langle R_N, \overline{\mathcal{M}[v_N]} \rangle = \int_{\Omega_N} \mu \nabla v_N \cdot \nabla \overline{\mathcal{M}[v_N]} + (1 - \lambda_N) \int_{\Omega_N} v_N \overline{\mathcal{M}[v_N]}. \tag{2.13}$$

Notice that in view of (2.8) and the definition of ψ_N , the sequence v_N is bounded in $H^1(\Pi)$:

$$\begin{aligned} \|\nabla v_N\|_{L^2(\Omega_N)} &\leq \|u_N \psi_N\|_{L^2(\Omega_N)}^{-1} (\|\nabla u_N\|_{L^2(\Omega_N)} + 4a_N^{-1} \|u_N\|_{L^2(\Omega_N)}) \\ &\leq \|u_N\|_{L^2(\omega_N)}^{-1} (c_4 + 4a_N^{-1}) \leq c_3^{-1} (c_4 + 4a_N^{-1}). \end{aligned} \tag{2.14}$$

Hence the sequence $\mathcal{M}[v_N]$ is bounded in $H^1(\Pi)$ as well, and the left-hand side of (2.13) converges to zero as $N \rightarrow \infty$, as follows from (2.7). Using this fact and (2.4) for the Bloch eigenfunctions V^k , we infer that

$$N \sum_{j=1}^N \sum_{k=1}^{\infty} h^k(j/N) |\alpha_N^{kj}|^2 (\lambda^k(j/N) - \lambda_N) \rightarrow 0 \tag{2.15}$$

as $N \rightarrow \infty$.

For a sequence $\{v_N^k\}_{k=1}^{\infty}$ of measures on $(0, 1]$ defined by

$$v_N^k(\theta) = N \sum_{j=1}^N |\alpha_N^{kj}|^2 \delta_{\theta=j/N},$$

where $\delta_{\theta=\theta_0}$ is the point mass at θ_0 , we have $\sum_{k=1}^{\infty} \int_0^1 dv_N^k(\theta) = 1$. For each $k \in \mathbb{N}$, up to selecting a subsequence, the sequence $\{v_N^k\}_{N=1}^{\infty}$ converges to some non-negative measure ν^k as $N \rightarrow \infty$. We claim that

$$\sum_{k=1}^{\infty} \int_0^1 d\nu^k(\theta) = 1. \tag{2.16}$$

Indeed, otherwise there exist $\delta > 0$ and $k_N \in \mathbb{N}$ such that $\sum_{k=k_N}^\infty \int_0^1 dv_N^k(\theta) \geq \delta$, or equivalently $N \sum_{k=k_N}^\infty \sum_{j=1}^N |\alpha_N^{kj}|^2 \geq \delta$ for each $N \in \mathbb{N}$. Then using (2.14), (2.12), the Plancherel theorem for $(\nabla + 2\pi i N^{-1} j e_1) v_N^j$ in terms of $(\nabla + 2\pi i N^{-1} j e_1) V^k(j/N, \cdot)$, $k \in \mathbb{N}$, and equation (2.4), yields for some $c_5 > 0$:

$$\begin{aligned} c_3(c_4 + 4a_N^{-1}) &\geq \|\nabla v_N\|_{L^2(\Omega_N)}^2 \\ &= N \sum_{j=1}^N \sum_{k=1}^\infty |\alpha_N^{kj}|^2 \|(\nabla + 2\pi i N^{-1} j e_1) V^k(j/N, \cdot)\|_{L^2(I_1 \times I_2)}^2 \\ &\geq c_5 N \sum_{k=1}^\infty \sum_{j=1}^N |\alpha_N^{kj}|^2 (\lambda^k(j/N) - 1) \geq c_5 \min_{\theta \in (0,1]} (\lambda^{k_N}(\theta) - 1) N \sum_{k=k_N}^\infty \sum_{j=1}^N |\alpha_N^{kj}|^2 \\ &\geq c_5 \delta \min_{\theta \in (0,1]} (\lambda^{k_N}(\theta) - 1) \xrightarrow{N \rightarrow \infty} \infty, \end{aligned}$$

which is impossible, hence (2.16) holds.

Finally, (2.15) implies

$$0 = \lim_{N \rightarrow \infty} \sum_{k=1}^\infty \int_0^1 h^k(\theta) (\lambda^k(\theta) - \lambda_N) dv_N^k(\theta) = \sum_{k=1}^\infty \int_0^1 h^k(\theta) (\lambda^k(\theta) - \lambda) dv^k(\theta),$$

from which, in view of (2.16) and the fact that the sequence $\{h^k\}_{k=1}^\infty$ is arbitrary, we immediately infer the existence of $k \in \mathbb{N}$ and $\theta \in (0, 1]$ such that $\lambda = \lambda^k(\theta)$, as required. \square

2.3 The lack of spectral pollution

Here we prove that no ‘boundary’ sequences of eigenvalues λ_N , as in Definition 1, converge to a limit outside the spectrum of the operator S defined via (2.6).

Theorem 2 *The boundary spectrum σ_{boundary} is contained in the set $\{\mu^{-1} : \mu \in \sigma_\Pi\}$, where σ_Π is the spectrum of the operator S .*

Proof Let $\lambda \in \sigma_{\text{boundary}}$ and consider a sequence of eigenvalues λ_N in the problem (2.1)–(2.2) that converges to λ and the sequence of associated eigenfunctions u_N , as in Definition 1.

We fix $0 < \gamma < 1$ and notice that there exists a sequence $\{N_j\}_{j=1}^\infty$ such that either $\|u_{N_j}\|_{L^2((0, N/2 - N_j^{7/2}) \times I_2)} \geq 1/4$ for any $j \in \mathbb{N}$ or $\|u_{N_j}\|_{L^2((N/2 + N_j^{7/2}, 1) \times I_2)} \geq 1/4$ for any $j \in \mathbb{N}$. Indeed, suppose the contrary, then there exists $N_0 \in \mathbb{N}$ such that for any $N \geq N_0$ one has $\|u_N\|_{L^2((0, N/2 - N^{7/2}) \times I_2)} < 1/4$, $\|u_N\|_{L^2((N/2 + N^{7/2}, 1) \times I_2)} < 1/4$ and $\|u_N\|_{L^2((N/2 - N^{7/2}, N/2 + N^{7/2}) \times I_2)} \leq \|u_N\|_{L^2((N/2 - N^{7/2}, N/2 + N^{7/2}) \times I_2)} < 1/4$, which is a contradiction with the fact that $\|u_N\|_{L^2(\Omega_N)} = 1$. Here we used the observation that we can take $a_N = N^\gamma$ in the definition of the boundary spectrum, hence

$$\|u_N\|_{L^2((N/2 - N^\gamma/2, N/2 + N^\gamma/2) \times I_2)} \rightarrow 0$$

as $N \rightarrow \infty$. In what follows we denote $\omega_N := (0, N/2 - N^{\gamma/2}) \times I_2$, assume without loss of generality that

$$\|u_{N_j}\|_{L^2(\tilde{\omega}_N)} \geq 1/4 \tag{2.17}$$

for any $j \in \mathbb{N}$, and use the notation u_N for the subsequence u_{N_j} .

Next, consider a sequence of smooth cut-off functions $\tilde{\psi}_N$ on \mathbb{R}_+ such that $\tilde{\psi}_N(x) = 1$ for $x \in (0, N/2 - N^{\gamma/2})$, $\tilde{\psi}_N(x) = 0$ for $x \in (N/2 - N^{\gamma/4}, \infty)$, and $|\tilde{\psi}'_N(x_1)| < 2N^{-\gamma/2}$ for any $x_1 \in \mathbb{R}_+$. In a similar fashion to the proof of Theorem 1, the functions

$$\tilde{v}_N(x) := \|u_N(\mathbf{x})\tilde{\psi}_N(x_1)\|_{L^2(\Omega_N)}^{-1} u_N(\mathbf{x})\tilde{\psi}_N(x_1)$$

extended by zero outside Ω_N , are well defined in Π , and $\|\tilde{v}_N\|_{L^2(\Pi)} = 1$. Moreover, for

$$\tilde{\mathcal{R}}_N := -\rho^{-1}(\mu\nabla\tilde{v}_N) + \tilde{v}_N - \lambda_N\tilde{v}_N,$$

one has

$$\|w_N\|_{H^1(\Pi)}^{-1} \langle \tilde{\mathcal{R}}_N, w_N \rangle \rightarrow 0 \tag{2.18}$$

as $N \rightarrow \infty$, for any sequence $w_N \in H^1(\Pi)$. Indeed, in the same way as in the proof of Theorem 1, $\|u_N\|_{H^1(\Omega_N)} \leq c_4$ for some $c_4 > 0$. Hence (2.17), the Cauchy–Schwarz inequality and the above bound for $|\tilde{\psi}'_N|$ yield

$$\begin{aligned} |\langle \tilde{\mathcal{R}}_N, w_N \rangle| &= \|u_N\psi_N\|_{L^2(\Omega_N)}^{-1} \left| \int_{\Pi} \mu\tilde{\psi}'_N(u_N(w_N)_{,x_1} - w_N(u_N)_{,x_1}) \right| \\ &= \|u_N\|_{L^2(\tilde{\omega}_N)}^{-1} c_2 \max_{x_1 \in \mathbb{R}_+} |\tilde{\psi}_N(x_1)| \|u_N\|_{H^1(\Omega_N)} \|w_N\|_{H^1(\Pi)} \leq 4c_2 2N^{-\gamma/2} c_4 \|w_N\|_{H^1(\Pi)}, \end{aligned}$$

which implies (2.18).

Further, since the sequence \tilde{v}_N is bounded in $H^1(\Pi)$, up to a subsequence it converges weakly in $H^1(\Pi)$ to some function \tilde{v} , which is found to satisfy the equation

$$-\rho^{-1}\nabla \cdot (\mu\nabla\tilde{v}) + \tilde{v} = \lambda\tilde{v}$$

in the weak sense. This follows immediately from the property (2.18) if one sets $w_N = w$ with a fixed but arbitrary function $w \in H^1(\Pi)$ and passes to the limit as $N \rightarrow \infty$.

Now, if $\tilde{v} \neq 0$ then λ^{-1} belongs to the point spectrum⁵ of S . If, on the contrary, $\tilde{v} = 0$, then \tilde{v}_N is a bounded and non-compact Weyl sequence for S , λ^{-1} , i.e. such that $\|S\tilde{v}_N - \lambda^{-1}\tilde{v}_N\| \rightarrow 0$ as $N \rightarrow \infty$. Indeed, consider the sequence of functions $\tilde{w}_N \in H^1(\Omega)$ satisfying

$$-\rho^{-1}\nabla \cdot (\mu\nabla\tilde{w}_N) + \tilde{w}_N = \tilde{v}_N$$

in the weak sense. Clearly,

$$-\rho^{-1}\nabla \cdot (\mu\nabla(\lambda^{-1}\tilde{v}_N - \tilde{w}_N)) + (\lambda^{-1}\tilde{v}_N - \tilde{w}_N) = (1 - \lambda^{-1}\lambda_N)\tilde{v}_N + \tilde{\mathcal{R}}_N,$$

in particular, using the above property of $\tilde{\mathcal{R}}_N$, one has $\|\lambda^{-1}\tilde{v}_N - \tilde{w}_N\|_{L^2(\Pi)} \rightarrow 0$ as $N \rightarrow \infty$. Hence λ^{-1} is an element of the continuous spectrum of S . \square

⁵ The point spectrum of S is defined as the set of values μ for which there is a non-zero $u \in H^1(\Pi)$ such that $Su = \mu u$.

2.4 Boundary two-scale convergence

In order to complete the proof of the fact that $\sigma_{\text{boundary}} \cup \sigma_{\text{Bloch}} = \sigma_{\Pi}$, it remains to obtain a lower semi-continuity-type inclusion $\sigma_{\Pi} \subset \lim_{N \rightarrow \infty} \sigma_N$ (see Section 2.5). It is known that the resolvent operator convergence leads to this kind of property (see e.g. Allaire & Conca, 1998b). In the setting we study here, the concept of resolvent two-scale operator convergence (see Zhikov, 2000) is especially useful, in view of the two-scale structure of the problem (2.1)–(2.2) as $N \rightarrow \infty$. We therefore introduce the notion of boundary two-scale convergence (cf. Allaire & Conca, 1998b), appropriate for our specific setting.

Henceforth we use the notation $Q := I_1 \times I_2$ for a ‘periodic unit cell’. Note that we will still write $I_1 \times I_2$ instead of Q whenever we treat $I_1 \times I_2$ as a macroscopic domain rather than a unit cell.

Definition 2 A sequence of functions $u_N \in L^2(I_1 \times I_2)$ is said to weakly boundary-two-scale (B2S) converge to a function $u \in L^2(\Pi)$ if for any $\varphi \in L^2(\Pi)$ one has

$$N \int_{I_1 \times I_2} u_N(x_1, x_2) \varphi(Nx_1, x_2) dx \rightarrow \int_{I_2} \int_{\mathbb{R}_+} u(x_1, x_2) \varphi(x_1, x_2) dx_1 dx_2 \quad (2.19)$$

as $N \rightarrow \infty$.

Remark 2 An analogous definition of weak B2S convergence of a sequence $u_N \in L^2(I_1)$ to $u \in L^2(\mathbb{R}_+)$ in one dimension would be

$$N \int_{I_1} u_N(x_1) \varphi(Nx_1) dx_1 \rightarrow \int_{\mathbb{R}_+} u(x_1) \varphi(x_1) dx_1$$

as $N \rightarrow \infty$, for any function $\varphi \in L^2(\mathbb{R}_+)$. Our case is, loosely speaking, ‘1.5-dimensional’.

Boundary-two-scale convergence, like the usual two-scale convergence (see Allaire, 1992; Nguetseng, 1989), has a version of the compactness property, which allows one to pass to the limit in boundary-value problems for multi-scale partial differential equations.

Theorem 3 Let u_N be a sequence of functions in $L^2(I_1 \times I_2)$ such that for some $c_6 > 0$ one has $N \|u_N\|_{L^2(I_1 \times I_2)}^2 \leq c_6$. Then there exists a subsequence u_{N_j} that weakly B2S converges to some function $u \in L^2(\Pi)$.

Proof For each $N \in \mathbb{N}$ consider the linear functional

$$L_N(\varphi) := N \int_{I_1 \times I_2} u_N(x_1, x_2) \varphi(Nx_1, x_2) dx,$$

for all $\varphi \in L^2(\Pi)$. Using the Cauchy–Schwarz inequality we deduce that

$$|L_N(\varphi)| \leq N \|u_N\|_{L^2(\Pi)} \left(\int_{I_1 \times I_2} |\varphi(Nx_1, x_2)|^2 dx \right)^{1/2} \leq c_7 \|\varphi\|_{L^2(\Pi)}$$

for some $c_7 > 0$. Hence, L_N is a bounded sequence of linear continuous functionals on the separable Banach space $L^2(\Pi)$ and thus there exists a sequence $\{N_j\}_{j=1}^\infty$ and a continuous functional L on $L^2(\Pi)$ such that

$$\lim_{j \rightarrow \infty} L_{N_j}(\varphi) = L(\varphi) \tag{2.20}$$

for any $\varphi \in L^2(\Pi)$. Since by the Riesz theorem there exists $u \in L^2(\Pi)$ such that $L(\varphi) = \int_\Pi u\varphi$, the definition of L_N and (2.20) imply (2.19). \square

In what follows we establish further useful properties of B2S convergence. These are analogous to the well-known results about the standard two-scale convergence (see Zhikov, 2000; Allaire, 1992).

Proposition 1 *If a sequence $u_n \in L^2(I_1 \times I_2)$ weakly B2S converges to a function $u \in L^2(\Pi)$ then a variant of the lower semi-continuity property holds: $\int_\Pi |u|^2 \leq \liminf_{N \rightarrow \infty} N \int_{I_1 \times I_2} |u_N|^2$.*

Proof Clearly, for any $N \in \mathbb{N}$, one has

$$\begin{aligned} 0 &\leq N \int_{I_1 \times I_2} (u_N(x_1, x_2) - u(Nx_1, x_2))^2 dx = N \int_{I_1 \times I_2} |u_N(x_1, x_2)|^2 dx \\ &\quad - 2N \int_{I_1 \times I_2} u_N(x_1, x_2)u(Nx_1, x_2)dx + N \int_{I_1 \times I_2} |u(Nx_1, x_2)|^2 dx. \end{aligned}$$

Taking the $\liminf_{N \rightarrow \infty}$ of both sides of this inequality yields

$$\begin{aligned} 0 &\leq \liminf_{N \rightarrow \infty} N \int_{I_1 \times I_2} |u_N(x_1, x_2)|^2 dx - 2 \lim_{N \rightarrow \infty} N \int_{I_1 \times I_2} u_N(x_1, x_2)u(Nx_1, x_2)dx \\ &\quad + \lim_{N \rightarrow \infty} N \int_{I_1 \times I_2} |u(Nx_1, x_2)|^2 dx = \liminf_{N \rightarrow \infty} N \int_{I_1 \times I_2} |u_N(x_1, x_2)|^2 dx - \int_{I_1 \times I_2} |u(x_1, x_2)|^2 dx, \end{aligned}$$

which implies the claim of the proposition. \square

Proposition 2 *If a sequence $u_N \in L^2(I_1 \times I_2)$ weakly B2S converges to a function $u \in L^2(\Pi)$ then for any bounded measurable function b defined on Π , the sequence $b(Nx_1, x_2)u_N(x_1, x_2)$ weakly B2S converges to bu .*

Proof The proposition is a direct consequence of the fact that if $\varphi \in L^2(\Pi)$ then $\tilde{\varphi} := b\varphi \in L^2(\Pi)$, which implies, for any $\varphi \in L^2(\Pi)$,

$$\begin{aligned} \int_{I_1 \times I_2} b(Nx_1, x_2)u_N(x_1, x_2)\varphi(Nx_1, x_2)dx &= \int_{I_1 \times I_2} u_N(x_1, x_2)\tilde{\varphi}(Nx_1, x_2)dx \\ &\xrightarrow{N \rightarrow \infty} \int_\Pi u(x)\tilde{\varphi}(x)dx = \int_\Pi b(x)u(x)\varphi(x)dx, \end{aligned}$$

as required. \square

Definition 3 A sequence of functions $u_N \in L^2(I_1 \times I_2)$ is said to strongly B2S converge to a function $u \in L^2(\Pi)$ if u_N weakly B2S converge to u and for any sequence $v_N \in L^2(I_1 \times I_2)$ that weakly B2S converges to a function $v \in L^2(\Pi)$, one has $N \int_{I_1 \times I_2} u_N v_N \rightarrow \int_{\Pi} uv$ as $N \rightarrow \infty$.

Proposition 3 If a sequence $u_N \in L^2(I_1 \times I_2)$ strongly B2S converges to a function $u \in L^2(\Pi)$ and b is a bounded measurable function defined on Π , then the convergence of the sequence $b(Nx_1, x_2)u_N(x_1, x_2)$ established in Proposition 2 is in fact strong.

Proof By Proposition 2, for any sequence $v_N \in L^2(I_1 \times I_2)$ that weakly B2S converges to $v \in L^2(\Pi)$ the sequence $\tilde{v}_N(x_1, x_2) = b(Nx_1, x_2)v_N(x_1, x_2)$ weakly B2S converges to $\tilde{v} := bv$. Hence,

$$\int_{I_1 \times I_2} b(Nx_1, x_2)u_N(x_1, x_2)v_N(x_1, x_2)dx = \int_{I_1 \times I_2} u_N \tilde{v}_N \xrightarrow{N \rightarrow \infty} \int_{\Pi} u \tilde{v} = \int_{\Pi} buv,$$

as required. \square

Proposition 4 Suppose that a sequence $u_N \in L^2(I_1 \times I_2)$ weakly B2S converges to a function $u \in L^2(\Pi)$. Then for this convergence to be strong in the sense of the above definition it is necessary and sufficient that

$$\int_{\Pi} |u|^2 \geq \limsup_{N \rightarrow \infty} N \int_{I_1 \times I_2} |u_N|^2. \quad (2.21)$$

Proof If $u_N \in L^2(I_1 \times I_2)$ strongly B2S converges to $u \in L^2(\Pi)$ then setting $v_N = u_N$ in the definition of the strong B2S convergence yields $\int_{I_1 \times I_2} u_N u_N \rightarrow \int_{\Pi} uu$, hence (2.21).

Conversely, suppose $u_N \in L^2(I_1 \times I_2)$ and $v_N \in L^2(I_1 \times I_2)$ weakly B2S converge to $u \in L^2(\Pi)$, and $v \in L^2(\Pi)$, respectively. Since $\sqrt{N}u_N$ and $\sqrt{N}v_N$ are bounded in $L^2(I_1 \times I_2)$, we can assume, after selecting a subsequence, that there exist finite limits $\lim_{N \rightarrow \infty} N \int_{I_1 \times I_2} u_N v_N$ and $\lim_{N \rightarrow \infty} N \int_{I_1 \times I_2} v_N^2$. Further, for any $t \in \mathbb{R}$, the sequence $v_N + tu_N$ weakly B2S converges to $v + tu$. Using Proposition 1,

$$\begin{aligned} & \lim_{N \rightarrow \infty} N \int_{I_1 \times I_2} v_N^2 + 2t \lim_{N \rightarrow \infty} N \int_{I_1 \times I_2} u_N v_N + t^2 \lim_{N \rightarrow \infty} N \int_{I_1 \times I_2} u_N^2 \\ &= \lim_{N \rightarrow \infty} N \int_{I_1 \times I_2} (v_N + tu_N)^2 \geq \int_{\Pi} (v + tu)^2 = \int_{\Pi} v^2 + 2t \int_{\Pi} uv + t^2 \int_{\Pi} u^2. \end{aligned}$$

Cancelling the terms $t^2 \lim_{N \rightarrow \infty} N \int_{I_1 \times I_2} u_N^2$ and $t^2 \int_{\Pi} u^2$ in view of (2.21), we get

$$\lim_{N \rightarrow \infty} N \int_{I_1 \times I_2} v_N^2 + 2t \lim_{N \rightarrow \infty} N \int_{I_1 \times I_2} u_N v_N \geq \int_{\Pi} v^2 + 2t \int_{\Pi} uv,$$

which is only possible if $\lim_{N \rightarrow \infty} N \int_{I_1 \times I_2} u_N v_N = \int_{\Pi} uv$, given that $t \in \mathbb{R}$ is arbitrary. \square

2.5 ‘Lower semi-continuity’ property for spectra

Here we focus on developing the ideas in relation to the resolvent operator convergence in our specific setting, as discussed at the beginning of Section 2.4.

Definition 4 We shall say that a sequence of operators S_N in $L^2(\Omega_N)$ strongly B2S converges to an operator S in $L^2(\Pi)$ if for any sequence f_N of functions defined on Ω_N , such that the sequence $\tilde{f}_N(x_1, x_2) := f_N(Nx_1, x_2)$ strongly B2S converges to a function $\tilde{f} \in L^2(\Pi)$, the sequence $(S_N f_N)(Nx_1, x_2)$ strongly B2S converges to the function $S\tilde{f}$.

For any operator S on $L^2(\Pi)$ we denote by $\sigma(S)$ its spectrum.

Theorem 4 If a sequence S_N strongly B2S converges to S then for any $\mu \in \sigma(S)$ there exists a sequence $\mu_N \in \sigma(S_N)$ such that $\mu_N \rightarrow \mu$ as $N \rightarrow \infty$.

Proof Suppose that the above claim does not hold. Then there exist $\mu \in \sigma(S)$ and $\kappa > 0$ such that $\text{dist}(\sigma(S_N), \mu) > \kappa$. Take $f \in L^2(\Pi)$ and denote by f_N the restriction of f to the domain Ω_N . Then, clearly, the sequence $f_N(Nx_1, x_2)$ strongly B2S converges to the function f . Hence,

$$\begin{aligned} \kappa \left(N \int_{I_1 \times I_2} |f_N(Nx_1, x_2)|^2 dx \right)^{1/2} &= \kappa \left(\int_{\Omega_N} |f_N(x)|^2 dx \right)^{1/2} \\ &= \kappa \|f_N\|_{L^2(\Omega_N)} \leq \|S_N f_N - \mu f_N\|_{L^2(\Omega_N)} \\ &= \sup_{\varphi \in L^2(\Omega_N)} \left(\int_{\Omega_N} |\varphi|^2 \right)^{-1/2} \left(\int_{\Omega_N} (S_N f_N - \mu f_N) \varphi \right) \\ &= \sup_{\varphi \in L^2(I_1 \times I_2)} \left(\int_{I_1 \times I_2} |\varphi(Nx_1, x_2)|^2 dx \right)^{-1/2} \\ &\quad \times \left(N \int_{I_1 \times I_2} (S_N f_N(Nx_1, x_2) - \mu f_N(Nx_1, x_2)) \varphi(Nx_1, x_2) dx \right). \end{aligned}$$

Passing to the limit as $N \rightarrow \infty$ yields

$$\begin{aligned} \kappa \|f\|_{L^2(\Pi)} &\leq \sup_{\varphi \in L^2(\Pi)} \left(\int_{I_2} \int_{\mathbb{R}_+} \varphi(x_1, x_2) dx_1 dx_2 \right)^{-1/2} \\ &\quad \times \left(\int_{I_2} \int_{\mathbb{R}_+} (Sf(x_1, x_2) - \mu f(x_1, x_2)) \varphi(x_1, x_2) dx_1 dx_2 \right) = \|Sf - \mu f\|_{L^2(\Pi)}, \end{aligned}$$

which, due to the fact that $f \in L^2(\Pi)$ is arbitrary, contradicts the assumption that $\mu \in \sigma(S)$. □

Theorem 5 For each $N \in \mathbb{N}$ define an operator S_N on $L^2(\Omega_N)$ by the formula $S_N f = u$, where for each $f \in L^2(\Omega_N)$ the function $u \in H^1(\Omega_N)$ is the solution to the problem (cf. (2.1)–(2.2))

$$\int_{\Omega_N} (\mu \nabla u \cdot \nabla \varphi + \rho u \varphi) = \int_{\Omega_N} \rho f \varphi$$

for any $\varphi \in H^1(\Omega_N)$. Then the operators S_N strongly B2S converge to the operator S .

Proof Consider a sequence of functions $f_N \in L^2(\Omega_N)$ such that $\tilde{f}_N(x_1, x_2) := f_N(Nx_1, x_2)$ strongly B2S converge to a function $\tilde{f} \in L^2(\Pi)$. Notice first that since

$$\|f_N\|_{L^2(\Omega_N)}^2 = N\|\tilde{f}_N\|_{L^2(I_1 \times I_2)}^2 \rightarrow \|\tilde{f}\|_{L^2(\Pi)}^2$$

as $N \rightarrow \infty$, there exists $c_8 > 0$ such that $\|f_N\|_{L^2(\Omega_N)}^2 < c_8$ for any $N \in \mathbb{N}$. Further, for $u_N = S_N f_N$ one has

$$\int_{\Omega_N} (\mu|\nabla u_N|^2 + \rho|u_N|^2) = \int_{\Omega_N} \rho f_N u_N. \tag{2.22}$$

By the Cauchy–Schwarz inequality, there exists $c_9 > 0$ such that $\|u_N\|_{L^2(\Omega_N)}^2 = N \int_{I_1 \times I_2} |u_N(Nx_1, x_2)|^2 dx < c_9$ for any $N \in \mathbb{N}$. Therefore, by the compactness principle, one can extract a subsequence u_{N_j} , for which we will keep the same notation u_N , such that the sequence $u_N(Nx_1, x_2)$ weakly B2S converges to a function $u \in L^2(\Pi)$.

Furthermore, (2.22) implies the existence of $c_{10} > 0$ such that $\|\nabla u_N\|_{L^2(\Omega_N)}^2 < c_{10}$ for all $N \in \mathbb{N}$, hence the sequence $U_N(Nx_1, x_2)$, where $U_N := \nabla u_N$, weakly B2S converges to a vector function $U \in [L^2(\Pi)]^2$.

Notice next that for a smooth function $\varphi = \varphi(x)$, $x \in \Pi$, with compact support and $N \in \mathbb{N}$ one has

$$\int_{\Omega_N} (\mu U_N \cdot \Phi + \rho u_N \varphi - \rho f_N \varphi) = 0, \tag{2.23}$$

where $\Phi := \nabla \varphi$. Rescaling (2.23) yields

$$N \int_{I_1 \times I_2} \{ \mu(Nx_1, x_2) U_N(Nx_1, x_2) \cdot \Phi(Nx_1, x_2) + \rho(Nx_1) u_N(Nx_1, x_2) \varphi(Nx_1, x_2) - \rho(Nx_1, x_2) f_N(Nx_1, x_2) \varphi(Nx_1, x_2) \} dx = 0,$$

from which, after passing to the limit as $N \rightarrow \infty$ and using the fact that $f_N(Nx_1, x_2)$ strongly B2S converge to the function \tilde{f} , we get

$$\int_{\Pi} (\mu U \cdot \Phi + \rho u \varphi - \rho \tilde{f} \varphi) = 0. \tag{2.24}$$

In view of the fact that $\Phi = \nabla \varphi$, the identity (2.24) is the weak formulation of the problem

$$-\rho^{-1} \nabla \cdot (\mu U) + u = \tilde{f}, \quad u \in H^1(\Pi).$$

Next we show that $\nabla u = U$, where the gradient of u is understood in the weak sense. Indeed, for $i = 1, 2$ and any smooth function φ on Π one has $\int_{\Omega_N} u_{N,i} \varphi = - \int_{\Omega_N} u_N \varphi_{,i}$. Rescaling to $I_1 \times I_2$ and passing to the two-scale limit yield $\int_{\Pi} U_i \varphi = - \int_{\Pi} u \varphi_{,i}$, which implies $u_{,i} = U_i$.

Finally, we show that the sequence u_N strongly B2S converges to u . According to Propositions 2 and 4, it is sufficient to check that

$$\limsup_{N \rightarrow \infty} N \int_{I_1 \times I_2} \rho(Nx_1, x_2) |u_N(Nx_1, x_2)|^2 dx \leq \int_{\Pi} \rho(x) |u(x)|^2 dx$$

as $N \rightarrow \infty$. To this end recall (2.22) and the identity

$$\int_{\Pi} (\mu|\nabla u|^2 + \rho|u|^2) = \int_{\Pi} \rho \tilde{f} u, \tag{2.25}$$

which is obtained above in the limit as $N \rightarrow \infty$. Since $f_N(Nx_1, x_2)$ and $u_N(Nx_1, x_2)$ strongly and weakly, respectively, B2S converge to \tilde{f} and u , the right-hand side of (2.22) converges to the right-hand side of (2.25) as $N \rightarrow \infty$. Hence, the left-hand side of (2.22) converges to the left-hand side of (2.25). Therefore,

$$\limsup_{N \rightarrow \infty} \int_{\Omega_N} \rho|u_N|^2 = \int_{\Pi} (\mu|\nabla u|^2 + \rho|u|^2) - \liminf_{N \rightarrow \infty} \int_{\Omega_N} \mu|\nabla u_N|^2.$$

Since by the weak B2S convergence of U_N to ∇u the inequality

$$\int_{\Pi} \mu|\nabla u|^2 \leq \liminf_{N \rightarrow \infty} \int_{\Omega_N} \mu|\nabla u_N|^2$$

holds, we conclude that

$$\limsup_{N \rightarrow \infty} \int_{\Omega_N} \rho|u_N|^2 \leq \int_{\Pi} \rho|u|^2.$$

□

Note that for each $N \in \mathbb{N}$ the set σ_N defined at the beginning of Section 2 is the spectrum of the operator S_N .

Corollary 1

$$\sigma_{\Pi} \subset \lim_{N \rightarrow \infty} \sigma_N,$$

where the limit is understood in the Hausdorff sense (see footnote 2).

2.6 Summary

Putting together the results of Sections 2.2, 2.3 and 2.5, we have

$$\lim_{N \rightarrow \infty} \sigma_N \subset \sigma_{\text{boundary}} \cup \sigma_{\text{Bloch}} \subset \sigma_{\Pi} \subset \lim_{N \rightarrow \infty} \sigma_N. \tag{2.26}$$

We obtain (2.26) by invoking Theorem 1 to give the first inclusion, Theorem 2 to give the second inclusion, and Corollary 1 to give the final inclusion. Since the leftmost and rightmost terms in (2.26) coincide, all terms in (2.26) are equal. This, in particular, implies the following statement.

Theorem 6 *As $N \rightarrow \infty$, the spectra σ_N converge in the Hausdorff sense to σ_{Π} . In other words, there is no ‘spectral pollution’ as $N \rightarrow \infty$: the limit of any convergent sequence of eigenvalues $\lambda = \lambda_N$ of the operators S_N is an element of the spectrum of S , and in this fashion all elements of the spectrum of S are obtained.*

Our analysis applies *mutatis mutandis* to the case where the governing equation (1.1) is supplied with boundary conditions (1.2) on top and bottom walls, but with a clamped boundary at the left end (Dirichlet data at $x_1 = 0$) and a freely vibration boundary at the right end (Neumann data at $x_1 = 1$). In that case, we obviously end up with a Bloch spectrum which is still given by (2.4)–(2.5). However, when handling the boundary spectrum via an analogue of Theorem 2 one has to invoke the union of two spectra for the operators defined by (2.6) where the semi-infinite strip Π is traction free at $x_1 = 0$ and then clamped at $x_1 = 0$. Accordingly, in this case σ_Π in (2.26) is replaced by the union of the two spectra.

3 A numerical study of the limiting problems: semi-infinite and finite strips

In the previous section we considered a thinning waveguide $\Sigma_\eta = (0, 1) \times (-\eta/2, \eta/2)$, $\eta > 0$, of fixed (unit) length, and were concerned with how its rescaled spectrum $\eta^2\sigma_\eta$ behaves in the limit as $\eta \rightarrow 0$. In (2.26) the limit spectrum was related to the spectrum σ_Π of a problem posed on $\Pi = \mathbb{R}_+ \times I_2$.

In this section we investigate numerically the mentioned problem on Π , and use the relationships developed in the above analysis to find part of σ_{boundary} . Our method is based on the idea of looking at only those elements of the point spectrum of the operator S defined in (2.6) that conform to a further restriction on the behaviour of solutions that decay as $x_1 \rightarrow \infty$, as follows.

Proposition 5 *The spectrum σ_Π contains all values λ for which there exists $\gamma \in \mathbb{C}$ with $\Re(\gamma) > 0$ such that the equation*

$$-\rho^{-1}(\nabla - \gamma \mathbf{e}_1)(\mu(\nabla - \gamma \mathbf{e}_1)v) = \lambda v$$

has a non-zero solution $v \in H_{\text{per}}^1(I_1 \times I_2)$ that satisfies $v_{,1} + \gamma v|_{x_1=0} = 0$ $x_2 \in I_2$. The related boundary-value problems are understood in the weak sense and by $H_{\text{per}}^1(I_1 \times I_2)$ we denote the closure of the set of infinitely smooth functions φ on $\overline{\Pi}$ that are 1-periodic in x_1 , which respect to the norm $\sqrt{\int_{I_1 \times I_2} (|\varphi|^2 + |\nabla\varphi|^2)}$.

Proof It follows immediately from the observation that given a function v with the above properties, the function $u(\mathbf{x}) = v(\mathbf{x})\exp(-\gamma x_1)$, $\mathbf{x} \in \Pi$, is an eigenfunction of the operator S . □

We further restrict our study to considering piecewise constant material parameters ρ and μ , which corresponds to a striped guide, such as that considered in Adams *et al.* (2008). In particular, we will be evaluating solutions of the equation

$$-\rho^{-1}(x_1)\nabla \cdot (\mu(x_1)\nabla u(\mathbf{x})) = \lambda u(\mathbf{x}), \quad (3.1)$$

where $\mathbf{x} \in \Pi$ in the infinite-length case, $\mathbf{x} \in (0, Nd) \times I_2$ in the finite-length case and $\mathbf{x} \in \mathbb{R}_+ \times \mathbb{R}$ in the infinite-height problem, and ρ and μ are d -periodic and piecewise constant. For generality, and to allow flexibility within the numerics, we introduce a

distance d for the cell length: this was set to unity within the previous sections. As noted in Adams *et al.* (2008), one could easily rewrite all this in the language of electromagnetism or acoustics.

3.1 Retrieving the governing equations in a dimensional setting

The analysis in the previous sections uses problem statements such as those for (1.1)–(1.3) that are already non-dimensional. To show how one arrives at these non-dimensional forms, and to connect with applications, we briefly consider a dimensional setting. The notation will, for definiteness, be taken to be that of elasticity, in particular that associated with shear horizontal (or ‘anti-plane shear’) polarisation. All variables and parameters with a tilde are dimensional. In the finite height case, we consider a striped guide occupying $-1/2 < \tilde{x}_2/\tilde{h} < 1/2$, $0 < \tilde{x}_1/\tilde{h} < L$, where $L \rightarrow \infty$ (a semi-infinite guide) is permitted.

Associated with the displacement \tilde{u} (perpendicular to the $(\tilde{x}_1, \tilde{x}_2)$ -plane) are the dimensional stresses $\tilde{\tau}_{ij}$ that in this polarisation, for $\tilde{\tau}_{i3}$, are simply

$$\tilde{\tau}_{i3} = \tilde{\mu} \frac{\partial \tilde{u}}{\partial \tilde{x}_i}, \quad i = 1, 2,$$

in each of the regions of constant material parameters, with $\tilde{\mu}$ denoting the dimensional shear modulus.

We consider a guide consisting of two materials, labelled 1 and 2, each characterised by a density $\tilde{\rho}$ and sound speed \tilde{c}_T that oscillate piecewise between $\tilde{\rho}^{(1)}, \tilde{c}_T^{(1)}$ and $\tilde{\rho}^{(2)}, \tilde{c}_T^{(2)}$, so that $\tilde{\mu}^{(1)} = \tilde{\rho}^{(1)}(\tilde{c}_T^{(1)})^2$ and $\tilde{\mu}^{(2)} = \tilde{\rho}^{(2)}(\tilde{c}_T^{(2)})^2$ are the shear moduli of the materials 1 and 2, respectively. Henceforth ‘ (j) ’ in the superscript denotes a material parameter, or variable, corresponding to, or only defined in, material j , for $j = 1, 2$.

We assume that material 1 occupies the regions $nd < \tilde{x}_1/\tilde{h} < nd + d^{(1)}$, and material 2 occupies the regions $nd + d^{(1)} < \tilde{x}_1/\tilde{h} < (n + 1)d \equiv nd + d^{(1)} + d^{(2)}$, for all non-negative integers n such that $(n + 1)d \leq L$. Further, for finite-length guides, L/d is constrained to be an integer, so that the guide contains an equal number of complete layers of each material. This constraint and Proposition 5 enable us to restrict the problem to the region $0 < \tilde{x}_1/\tilde{h} < d$ subject to the Bloch-type conditions enforcing decay as $\tilde{x}_1 \rightarrow \infty$.

Conditions on the guide walls, $\tilde{x}_2/\tilde{h} = \pm 1/2$, are set to be both either traction-free or clamped. The edges $\tilde{x}_1/\tilde{h} = 0$, and $\tilde{x}_1/\tilde{h} = L$ for finite guides, are subject to either traction-free or clamped conditions, but these need not be the same as those at $\tilde{x}_2/\tilde{h} = \pm 1/2$.

We non-dimensionalise throughout using parameters of material 1 by introducing the following non-dimensional variables and parameters:

$$\begin{aligned} x_1 = \tilde{x}_1/\tilde{h}, \quad x_2 = \tilde{x}_2/\tilde{h}, \quad t = \tilde{c}_T^{(1)}\tilde{t}/\tilde{h}, \quad u = \tilde{u}/\tilde{h}, \quad \tau_{ik} = \tilde{\tau}_{ik}/(\tilde{\rho}^{(1)}(\tilde{c}_T^{(1)})^2), \\ \omega = \tilde{h}\tilde{\omega}/\tilde{c}_T^{(1)}, \quad \alpha^{(j)} = \tilde{c}_T^{(j)}/\tilde{c}_T^{(1)}, \quad \beta^{(j)} = \tilde{\rho}^{(j)}/\tilde{\rho}^{(1)}, \end{aligned}$$

for $j = 1, 2$, and everything hereafter is non-dimensional.

3.2 Application of the modal method

We have non-dimensionalised the problem in the previous section so as to retrieve the governing equations posed in the analysis, and imposed the restriction that the material parameters vary in a piecewise constant fashion to coincide with the striped guide considered in Adams *et al.* (2008). Figure 1(d) shows the set-up of the non-dimensional problem on Π .

The governing Helmholtz equation can now be cast as

$$(\alpha^{(j)})^2 \left(\frac{\partial^2 u^{(j)}}{\partial x_1^2} + \frac{\partial^2 u^{(j)}}{\partial x_2^2} \right) + \omega^2 u^{(j)} = 0,$$

valid within the domains occupied by materials $j = 1, 2$, and connected by continuity conditions at the interface, which are developed below. Note that λ in (3.1) is identified with ω^2 . Expressions for the stresses in terms of the displacement are

$$\tau_{13}^{(j)} = \beta^{(j)} (\alpha^{(j)})^2 \frac{\partial u^{(j)}}{\partial x_1}, \quad \tau_{23}^{(j)} = \beta^{(j)} (\alpha^{(j)})^2 \frac{\partial u^{(j)}}{\partial x_2}.$$

Traction-free boundary conditions, $\tau_{23} = 0$, or clamped boundary conditions, $u = 0$, are applied along the guide walls $x_2 = \pm 1/2$. Conditions on the edge, $x_1 = 0$, are also either traction-free, $\tau_{13} = 0$, or clamped, $u = 0$. Interface conditions ensuring the continuity of normal-stress and displacement at material junctions are imposed:

$$u^{(1)}|_{x_1=x_{1^*}^-} = u^{(2)}|_{x_1=x_{1^*}^+}, \quad \tau_{13}^{(1)}|_{x_1=x_{1^*}^-} = \tau_{13}^{(2)}|_{x_1=x_{1^*}^+}, \quad (3.2)$$

for $x_{1^*} = md, md + d^{(1)}$, $m \in \mathbb{N} \cup \{0\}$. Henceforth a superscript ‘+’ (‘-’) is used with field variables on the right (left) side of interface. Notice that the conditions (3.2) follow from the weak formulation, (1.4).

Using Proposition 5, or its appropriate analogue in the case of clamped edges and/or guide walls, we look for values λ for which there exist non-zero u satisfying

$$-\rho^{-1}(x_1) \nabla \cdot (\mu(x_1) \nabla u(x)) = \lambda u(x), \quad \mathbf{x} \in \mathbb{R}_+ \times I_2,$$

subject to the conditions:

(1) There exists $\gamma \in \mathbb{C}$, $\Re(\gamma) > 0$, such that for any $m \in \mathbb{N} \cup \{0\}$:

$$u((m+1)d, x_2) = u(md, x_2) \exp(-\gamma d), \quad x_2 \in I_2, \quad (3.3)$$

$$\tau_{13}((m+1)d, x_2) = \tau_{13}(md, x_2) \exp(-\gamma d) \quad x_2 \in I_2. \quad (3.4)$$

(2) The condition $u(0, x_2) = 0$, $x_2 \in I_2$, in the case when the edge $x_1 = 0$ is clamped and $\tau_{13}(0, x_2) = 0$, $x_2 \in I_2$, when it is traction-free.

(3) The appropriate (Dirichlet or Neumann) conditions at the horizontal parts of the boundary, $x_2 = -1/2$ and $x_2 = 1/2$.

Due to (2.26), the accessible elements of σ_{boundary} are thus associated with eigensolutions that decay exponentially as $x_1 \rightarrow \infty$, are defined by their behaviour on the cell, $(0, d) \times I_2$, via the relations (3.3)–(3.4), and do not belong to σ_{Bloch} .

Consider a single-mode solution in each of the materials, of the form:

$$u^{(j)}(x_1, x_2) = [A_n^{(j)} \exp(ik_n^{(j)}x_1) + B_n^{(j)} \exp(-ik_n^{(j)}x_1)]\hat{u}_n^{(j)},$$

valid for $k_n^{(j)} \neq 0$, in which $A^{(j)}, B^{(j)}, j = 1, 2$, are constants, and $\hat{u}_n^{(j)}$ is the n th modal solution to the homogeneous problem:

$$\hat{u}_n^{(j)}(x_2) = \begin{cases} \cos [n\pi(x_2 + 1/2)], \\ \sin [n\pi(x_2 + 1/2)], \end{cases} \quad \hat{\tau}_{13n}^{(j)}(x_2) = i\beta^{(j)}(\alpha^{(j)})^2 k_n^{(j)} \begin{cases} \cos [n\pi(x_2 + 1/2)], \\ \sin [n\pi(x_2 + 1/2)], \end{cases} \quad (3.5)$$

where

$$k_n^{(j)} = \sqrt{(\alpha^{(j)})^{-2}\omega^2 - n^2\pi^2}, \quad j = 1, 2, \quad n = \begin{cases} 0, 1, 2, \dots, \\ 1, 2, 3, \dots \end{cases}$$

In the above formulae, the upper (lower) terms in curly brackets refer to the Neumann/traction-free (Dirichlet/clamped) cases. The main difference between the clamped and traction-free cases is the exclusion of $n = 0$ in the clamped case. In the traction-free case, $n = 0$ leads to a constant solution for $\hat{u}_n^{(j)}$, whereas in the clamped case this corresponds to the trivial solution and is hence omitted.

Remark 3 Provided that the conditions on the boundaries of the guide are homogeneous, a no mode-conversion property (monomode property as referred to in the physics community) at the interfaces can readily be shown, as in Adams *et al.* (2008): an incoming mode is only transmitted and reflected into the same mode. Since modes do not interact, we can consider only a single mode rather than a (non-finite) sum of modes. We drop the notation n in subscript and assume henceforth that all variables and parameters correspond to the n th modal solution only, but return to this point in our discussion of stop-bands.

We call on the matrix-based techniques as in Pagneux & Maurel (2002). Within a homogeneous section of guide the wave field corresponding to a single mode is written as

$$\begin{pmatrix} \tau_{13}^{(j)}(x_1, x_2) \\ u^{(j)}(x_1, x_2) \end{pmatrix} = \begin{pmatrix} a^{(j)}(x_1)\hat{\tau}_{13}^{(j)}(x_2) \\ b^{(j)}(x_1)\hat{u}^{(j)}(x_2) \end{pmatrix}.$$

Here we denote $a^{(j)}(x_1) = ik^{(j)}(A^{(j)} \exp(ik^{(j)}x_1) - B^{(j)} \exp(-ik^{(j)}x_1))$ and $b^{(j)}(x_1) = A^{(j)} \exp(ik^{(j)}x_1) + B^{(j)} \exp(-ik^{(j)}x_1)$. The amplitudes in front of $\exp(ik^{(j)}x_1)$ and $\exp(-ik^{(j)}x_1)$ represent the contribution by the n th modal solution in the right- and left-going directions respectively. The angle θ made in the complex plane by $k^{(j)}$ and the positive real-axis satisfies $0 \leq \theta \leq \pi/2$.

Invoking continuity of normal stress and displacement across a material interface at $x_1 = x_{1*}$, one can equate these to yield:

$$\begin{pmatrix} a^-(x_{1*})\hat{\tau}_{13}^-(x_2) \\ b^-(x_{1*})\hat{u}^-(x_2) \end{pmatrix} = \begin{pmatrix} a^+(x_{1*})\hat{\tau}_{13}^+(x_2) \\ b^+(x_{1*})\hat{u}^+(x_2) \end{pmatrix}.$$

Examining (3.5), and recalling that the dependence of $\hat{u}^{(j)}$ and $\hat{\epsilon}_{13}^{(j)}$ on material parameters j is only through a scalar factor, we obtain $\beta^{(2)}(\alpha^{(2)})^2 k^{(2)} a^{(2)} = \beta^{(1)}(\alpha^{(1)})^2 k^{(1)} a^{(1)}$ and $b^{(2)} = b^{(1)}$. The Floquet–Bloch-type conditions (3.3)–(3.4) are equivalent to $a^{(1)}(d) = a^{(1)}(0) \exp(-\gamma d)$, $b^{(1)}(d) = b^{(1)}(0) \exp(-\gamma d)$. We combine this with results for a homogeneous material, found in Pagneux & Maurel (2002), to arrive at

$$\exp(-\gamma d) \begin{pmatrix} a^{(1)}(0) \\ b^{(1)}(0) \end{pmatrix} = \begin{pmatrix} a^{(1)}(d) \\ b^{(1)}(d) \end{pmatrix} = \mathcal{M} \begin{pmatrix} a^{(1)}(0) \\ b^{(1)}(0) \end{pmatrix}, \quad (3.6)$$

$$\mathcal{M} = \begin{pmatrix} \mathcal{C}^{(2)} & i\mathcal{S}^{(2)} \\ i\mathcal{S}^{(2)} & \mathcal{C}^{(2)} \end{pmatrix} \begin{pmatrix} r^{-1} & 0 \\ 0 & 1 \end{pmatrix} \begin{pmatrix} \mathcal{C}^{(1)} & i\mathcal{S}^{(1)} \\ i\mathcal{S}^{(1)} & \mathcal{C}^{(1)} \end{pmatrix} \begin{pmatrix} r & 0 \\ 0 & 1 \end{pmatrix}, \quad (3.7)$$

where $\mathcal{C}^{(j)} := \cos(k^{(j)}d^{(j)})$, $\mathcal{S}^{(j)} := \sin(k^{(j)}d^{(j)})$ and $r := k^{(2)}\beta^{(2)}(\alpha^{(2)})^2/k^{(1)}\beta^{(1)}(\alpha^{(1)})^2$.

Examining (3.6), we require $a^{(1)}(0) = 0$ when the edge $x_1 = 0$ is subject to traction-free conditions, and $b^{(1)}(0) = 0$ when it is clamped. Clearly, imposing these conditions will also satisfy the problem for a strip of finite length. Requiring non-trivial solutions, results in the following two simultaneous equations for ω and γ :

$$0 = \begin{cases} r^{-1}\mathcal{C}^{(2)}\mathcal{S}^{(1)} + \mathcal{S}^{(2)}\mathcal{C}^{(1)}, \\ r\mathcal{C}^{(2)}\mathcal{S}^{(1)} + \mathcal{S}^{(2)}\mathcal{C}^{(1)}, \end{cases} \quad (3.8)$$

$$\exp(-\gamma d) = \begin{cases} \mathcal{C}^{(2)}\mathcal{C}^{(1)} - r^{-1}\mathcal{S}^{(2)}\mathcal{S}^{(1)}, \\ \mathcal{C}^{(2)}\mathcal{C}^{(1)} - r\mathcal{S}^{(2)}\mathcal{S}^{(1)}, \end{cases} \quad (3.9)$$

where the upper (lower) terms in curly brackets refer to the case of traction-free (clamped) conditions on $x_2 = \pm 1/2$. Clearly, the pair of equations in (3.9) are identical up to the replacement of r by r^{-1} . Hence, the only difference between the two cases is the exclusion of $n = 0$ from the clamped problem, which leads to a zero-frequency band gap (Poulton *et al.*, 2001); the monomode property ensures that conditions imposed have no other influence on the solution, which is otherwise determined by the condition(s) imposed on the left (and right for a finite-length guide) edge(s). Standard root-finding techniques are employed on (3.8) and solutions form a list of candidate frequencies. The corresponding ‘Bloch parameters’ $-i\gamma$ are then immediate from (3.9), and only those solutions with $\Re(\gamma) > 0$ are physically meaningful.

Remark 4 In the case of an infinite guide, considered in Adams *et al.* (2008), (3.9) is posed as an eigenvalue problem. Propagating solutions are sought, and the notation $k_0 = -i\gamma$ is used to describe the phase change over each cell: all frequencies, with the exception of those in a stop-band, correspond to real Bloch parameters k_0 , and so support energy propagation through the guide. These Bloch solutions also hold for the semi-infinite strip as the eigenfunctions are arbitrary to within a multiplicative constant/phase shift and this can be chosen to satisfy the edge conditions as the guide is monomode, see (3.9). Thus numerically one finds that the spectrum consists of this continuous spectrum coupled with the discrete spectrum.

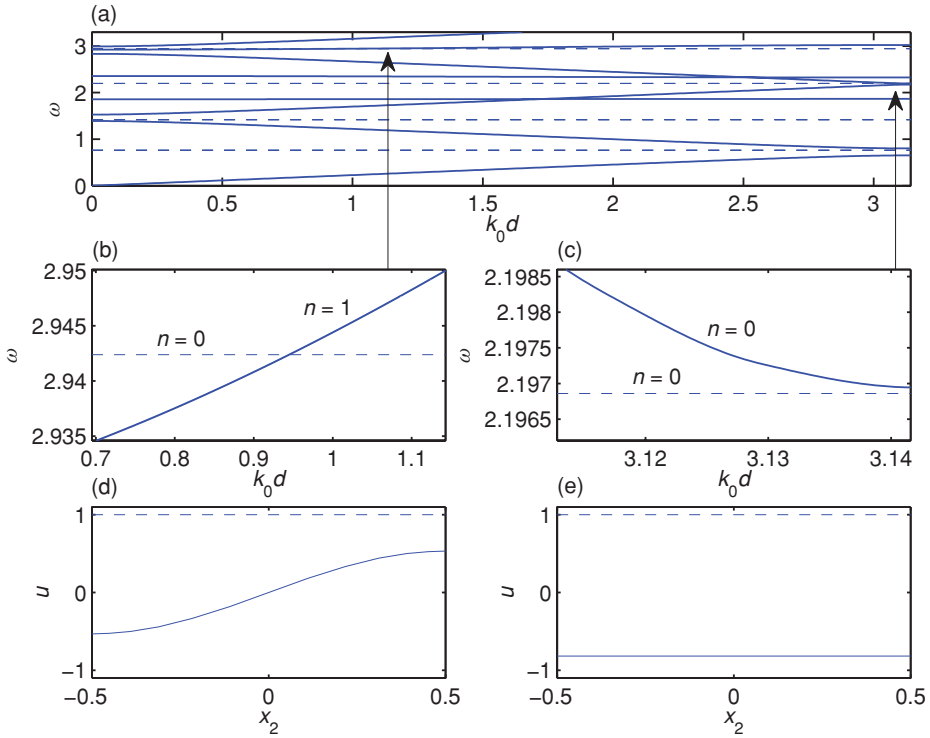


FIGURE 2. (Colour online) (a) Dispersion curves for surface modes corresponding to a single value of $\gamma = -ik_0$ and which form part of the point spectrum of S are shown as dashed curves, and the Bloch spectrum, σ_{Bloch} , for the analogous infinite case as the solid lines. (b) Surface waves and modes of the infinite structure can coincide away from the edges of the Brillouin zone; investigation shows this is only possible when the wavenumbers across the guide differ. These wavenumbers are indexed by n , which counts the number of half-oscillations across the guide, and are shown in (b) and (c). We draw attention to the fact that the surface modes exist within the gaps created by the infinite problem at the edges of the Brillouin zone, by zooming in on a band in (c), which shows that the surface wave lies extremely close to the upper mode, but still within the gap. Panels (d) and (e) show the corresponding mode shapes for the crossing, in (b) and the near crossing, in (c). When n differs, crossing can be observed, but for n the same, crossing cannot be observed.

We now examine three problems; first we deal with guides of finite height and use the aforementioned method to find elements in σ_{boundary} . We compare these results to the spectrum σ_{Bloch} for the problem dealt with in Adams *et al.* (2008), and note how these spectra interact. To extend the results and to gain insight into the finite height problem, we consider a guide of infinite height. In this instance, we no longer have an integer n by which we can index the solutions, and instead we have a continuous wavenumber k_{x_2} . We then use these results to develop a link between the elements the method obtains in σ_{boundary} and the spectrum σ_{Bloch} .

3.3 Results: Finite-height guides

Figure 2 shows the solutions for the infinite case, in which k_0 measures the phase change across the cell, as solid curves. Also shown on the figure are the surface mode frequencies,

Table 1. The first 10 surface mode frequencies and corresponding Bloch values for an Aluminium(1)–Tin(2) guide, subject to traction-free conditions on the edge $x_1 = 0$. The number of half-oscillations across the guide is given by n , and so gives the parity of the surface modes. (a) The first 10 values in the case when the guide is traction-free on $x_2 = \pm 1/2$; when it is clamped on $x_2 = \pm 1/2$, $n = 0$ must be excluded, and the first 10 values are shown in (b)

ω	γ	n
(a) The traction-free case		
0.7624	0.0470–0.5236i	0
1.4168	0.0392	0
2.1968	0.0010–0.5236i	0
2.9424	0.0536	0
3.3038	0.2300–0.5236i	1
3.6012	0.0308–0.5236i	0
3.7556	0.0002	1
4.3618	0.1023–0.5236i	1
4.3930	0.0040	0
4.9052	0.0226	1
(b) The clamped case		
3.3038	0.2300–0.5236i	1
3.7556	0.0002	1
4.3618	0.1023–0.5236i	1
4.9052	0.0226	1
5.6538	0.0305–0.5236i	1
6.2428	0.0721	1
6.3500	0.2499–0.5236i	2
6.5446	0.0126	2
6.9418	0.0010–0.5236i	1
7.0188	0.1739–0.5236i	2

shown as dashed horizontal lines; and these occur at discrete, complex, values of $k_0 = i\gamma$, and thus the k_0d axis is irrelevant here. The guide layers are Aluminium ($c_T = 3130 \text{ ms}^{-1}$), material 1; and Tin ($c_T = 1670 \text{ ms}^{-1}$), material 2; henceforth referred to as Aluminium(1)–Tin(2). Conditions on the guide walls and on the edge $x_1 = 0$ are Neumann, and the layer widths are $d^{(1)} = d^{(2)} = 3$. The first 10 frequency-Bloch parameter pairs are given in Table 1.

Whenever there is a non-trivial imaginary component of γ it is equal to $-\pi/d$, equivalent to a phase change of π over one layer. In these cases, the cell is effectively of length $2d$, and the phase changes across the first two layers and the second two cancel. By considering instead a unit cell of length $2d$, we would obtain a real Bloch parameter equal to $2\Re(\gamma)$. We note further that decay occurs over a scale of $(\Re(\gamma)d)^{-1}$ layers, whose value can be large, for example, the seventh surface mode decays over $(\Re(\gamma)d)^{-1} \sim 800d$ length units.

Results for the clamped case with a traction-free condition on edge $x_1 = 0$ are the same but exclude $n = 0$ values. Figures 2(b) and 2(c) show a zoom of Figure 2(a), indicated by arrows. We observe that on the edge of the Brillouin zone, at $k_0d = 0, \pi$, surface waves

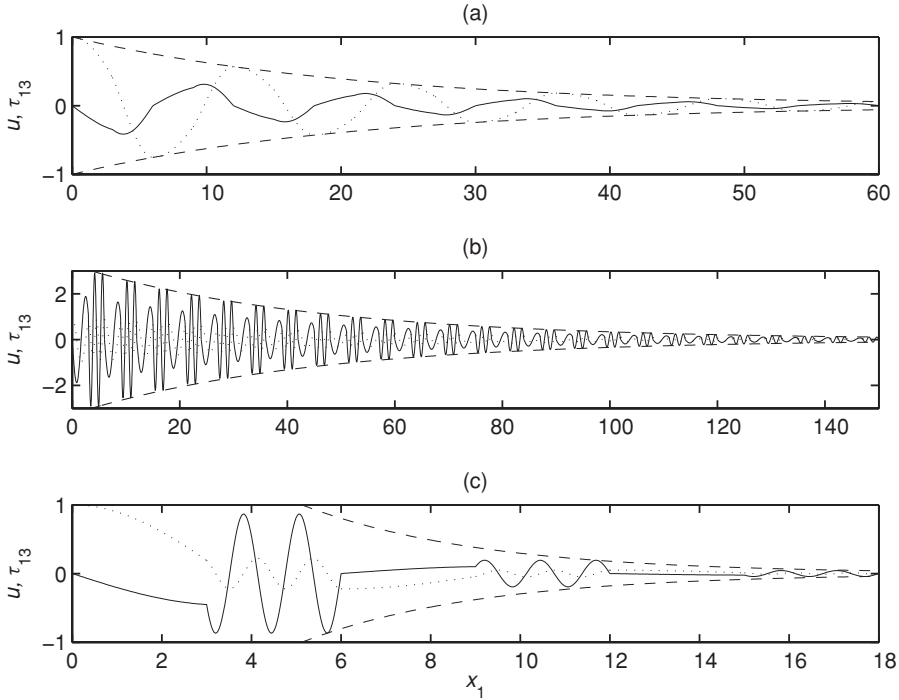


FIGURE 3. Stress τ_{13} , shown as solid curves, and displacement, shown as dotted curves, mode shapes for surface modes, normalised to have unit displacement at $x_1 = 0$ of the Aluminium(1)–Tin(2) guide, with traction-free edge conditions. Panel (a) corresponds to $\omega = 0.7642$, with $n = 0$. This mode, unlike (b) and (c), only exists in the traction-free problem. Panel (b) corresponds to $\omega = 4.9052$, $n = 1$. Panel (c) corresponds to $\omega = 6.35$, $n = 2$. Also plotted are the decay envelopes, shown as dashed curves, which bound the mode shapes and dictate its decay.

(dashed lines) lie within gaps created by nearby modes, and further investigation shows that those modes nearby have the same shape across the guide as the surface wave. We later demonstrate in a special case of weak material contrast between layers that this always holds: for a given value of n (which counts the number of half-oscillations across the guide): surface waves with n half-oscillations across the guide do not intersect modes with the same n , as in (3.5). However, when these n values differ between the guide, the surface wave, and mode of the infinite structure, as they do in Figure 2(b), a crossing within the Brillouin zone is possible, as shown. Nonetheless for the full spectrum, as illustrated by Figure 2(a), we emphasise that there are eigenvalues present that are not contained within σ_{Bloch} .

Figure 3 shows a selection of stress and displacement mode shapes in the Aluminium(1)–Tin(2) guide with a traction-free edge condition, as considered in Figure 2. Frequencies, ω , and mode numbers, n , are given in the caption; and corresponding Bloch values are found in Table 1. We draw particular attention to Figure 3(c), which demonstrates that in cases when γ has imaginary part equal to $-\pi/d$ (in this case, $\gamma = 0.25 - 0.52i$), the phase shifts by π over a cell. We also sketch the decay envelopes, proportional to $\exp(-\Re(\gamma)x)$, to illustrate how the mode shapes decay as $x \rightarrow \infty$. One can see from Table 1 that there is

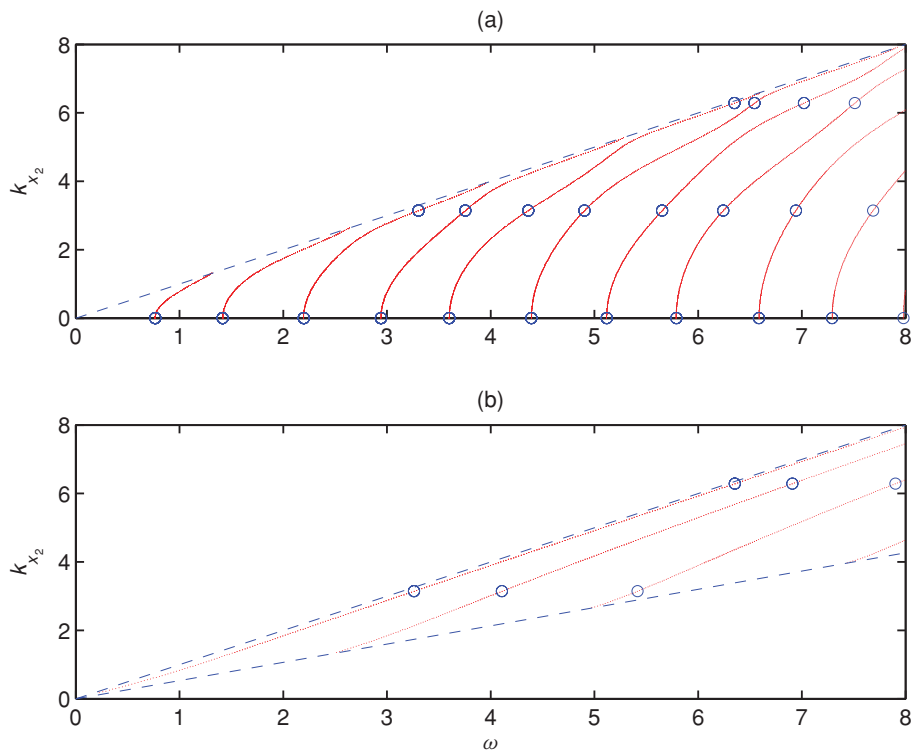


FIGURE 4. (Colour online) Dispersion curves for a problem in which the layers are of infinite height, and travel in x_2 is governed by wavenumber k_{x_2} , when the edge $x_1 = 0$ is traction-free. Panel (a) is for the Aluminium(1)–Tin(2) guide, and (b) is for a Tin(1)–Aluminium(2) guide. Circled in the figure are the instances when this coincides with the finite height guide, those $k_{x_2} = n\pi/2$ for n integer. The dashed curves sketched show the bulk wave solutions, $k_{x_2} = \omega/c_T^{(j)}$. In each case, the surface modes are confined to have phase speed greater than the bulk speed of material 1. In (b), the bulk speed of material 2 also bounds the surface modes.

large variation in decay length scales; the first 10 surface modes decay over length scales ranging from 1d to 800d. Drawing attention to the fact that the modal solutions satisfy the traction-free edge conditions for all $x_1 = nd$ for integer n , as shown in the figure, we note that mode shapes would be unchanged for any truncation of the semi-infinite guide whose length is an integer multiple of d .

3.4 Results: Infinite-height guides

We consider a related problem in which the guide is of infinite height, as in Camley *et al.* (1983), to provide insight into the finite thickness guide considered herein. Assuming a wavenumber k_{x_2} in the x_2 direction, it is clear that solutions for the infinite-height problem and finite-height problem coincide whenever $k_{x_2} = m\pi/2$ for integer m . Figures 4 and 5 show dispersion curves for guides in which the edge $x_1 = 0$ is traction-free and clamped respectively. An Aluminium(1)–Tin(2) guide is treated in Figure 4(a), a Tin(1)–Aluminium(2) guide in Figure 4(b), a Steel(1)–Lead(2) guide in Figure 5(a) and

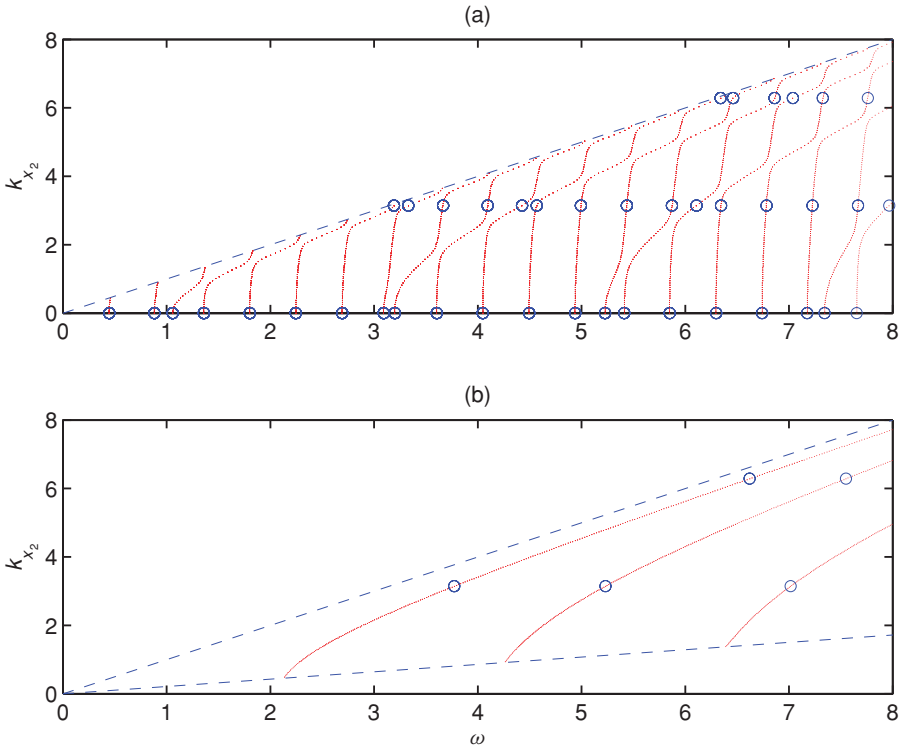


FIGURE 5. (Colour online) Dispersion curves a problem with infinite height layers in which travel in x_2 is governed by wavenumber k_{x_2} and edge $x_1 = 0$ is clamped. Panel (a) is for the Steel(1)–Lead(2) guide, and panel (b) is for a Lead(1)–Steel(2) guide. Circled in the figure are the instances when this coincides with the finite height guide. Dashed curves sketched show the bulk wave solutions, $k_{x_2} = \omega/c^{(j)}$. As in the free-edge case, the surface modes are confined to have phase speed greater than the bulk speed of material 1. In (b), the bulk speed of material 2 also bounds the surface modes.

a Lead(1)–Steel(2) guide in Figure 5(b). Those k_{x_2} corresponding to solutions for the guide problem are circled in each panel. The dashed curves correspond to the bulk modes in each material, with wavenumber $k_{x_2} = \omega/c_T$. In both cases, the surface modes have phase speed bounded below by the bulk wave speed of the material in contact with the edge, material 1. Further, in Figures 4(b) and 5(b), in which the wave speed of material 2 is greater than that of material 1, the bulk speeds of material 2 bounds the solutions, and as a result, far fewer solutions are available. In particular, $n = 0$ yields no solutions and so the frequency spectrum in the clamped and traction-free cases are the same in this instance. If the wave speed of material 1 is greater than that of material 2, $\alpha^{(2)} < 1$, as in Figures 4(a) and 5(a), surface modes solutions are always available at $n = 0$.

It is worth noting also that cases arise in which the bulk speed of the outer material (1) is lower than that of inner material (2), as treated in Figures 4(b) and 5(b), but in which modal solutions exist with phase speed above the bulk speed in both layers. In this instance, a repulsion phenomena is observed, and modes asymptote to the faster bulk

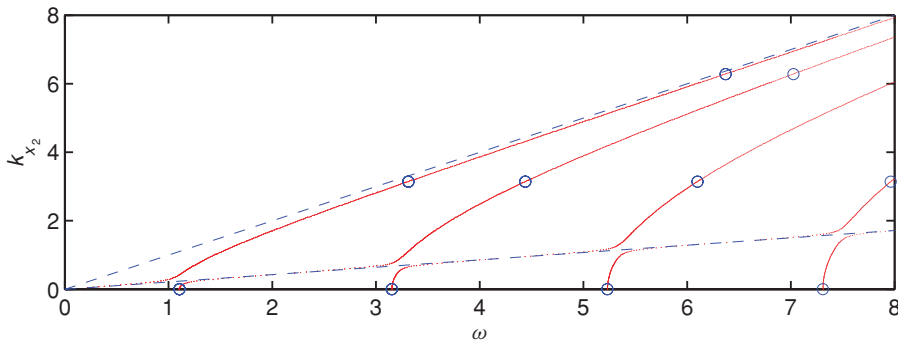


FIGURE 6. (Colour online) Dispersion curves for a problem with infinite height and edge $x_1 = 0$ is traction-free, for the Lead(1)–Steel(2) guide. Circled in the figure are those instances which coincide with the finite height guide. Dashed curves sketched show the bulk wave solutions, $k_{x_2} = \omega/c^{(j)}$. We draw attention to those modes which exist above the bulk speed of the faster materials, below the lower dashed curve, and observe the repulsion phenomena between modes at the bulk band interface.

speed (of material 2), before continuing into the region bounded by both bulk speeds; such curves are ultimately still bounded below by the bulk speed of the slower material (1). Figure 6 shows an example of this when the $x_1 = 0$ edge is traction-free, for a Lead–Steel guide of the same dimensions as considered in Figures 4 and 5. We now examine changes as the layer thickness varies, and in doing so provide a method by which one could tune the guide to achieve the desired response. Figure 7 shows the surface modes of an Aluminium(1)–Tin(2) guide for $n = 1$ in Figure 7(a) and $n = 2$ in Figure 7(b), in which the edge $x_1 = 0$ is traction-free. The cell width is $d = 6$, as in previous examples, and is held constant while layer thicknesses, $d^{(1)}, d^{(2)}$, are varied. There are a number of discrete values of $d^{(1)}$, as modes in material 1 become cut-on, with $k^{(1)} = 0$. Those cut-on ω and $d^{(1)}$ values can be obtained when $c_T^{(1)} > c_T^{(2)}$, as is the case here, by noting that $k^{(1)} = 0$ and the surface wave relation implies that $k^{(2)}d^{(2)} = m\pi$ for integer m ; and this yields $d^{(1)} = d - d^{(2)} = d - 2m/n\sqrt{(\alpha^{(2)})^{-2} - 1}$. This occurs at $\omega = n\pi$ and is indicated by a dashed horizontal line, and cut-on values of $d^{(1)}$ are circled. The cut-off frequency in the faster material bounds frequencies from below, which are unbounded above for all n . For $n = 0$, modes are bounded below by $\omega = 2\alpha^{(2)}\pi/d$, which is achieved only at $d^{(1)} = 0$, equivalent to the homogeneous guide case.

Figure 8 shows the analogous results for a guide of the same total length, composed of Tin(1)–Aluminium(2), for which $c_T^{(1)} < c_T^{(2)}$. Cut-off ω and $d^{(1)}$ can be similarly obtained by noting that $k_2 = 0$ and thus $d^{(1)} = 2m/n\sqrt{(\alpha^{(2)})^{-2} - 1}$. The cut-off frequency in the slower (outer) material is the lower bound, which is never achieved, and is shown by a dashed line in the figure. In this particular case, the material 2 cut-off frequency forms an upper bound, and $(d^{(1)}, \omega)$ values are circled in the figure. This is not universally the case, as some choices of materials permit the existence of surface modes of unbounded frequency for each n . In such cases, for example, a Lead–Steel guide of the same dimensions, surface modes go through the cut-off frequencies at $(d^{(1)}, \omega)$ given above, and are unbounded for each n .

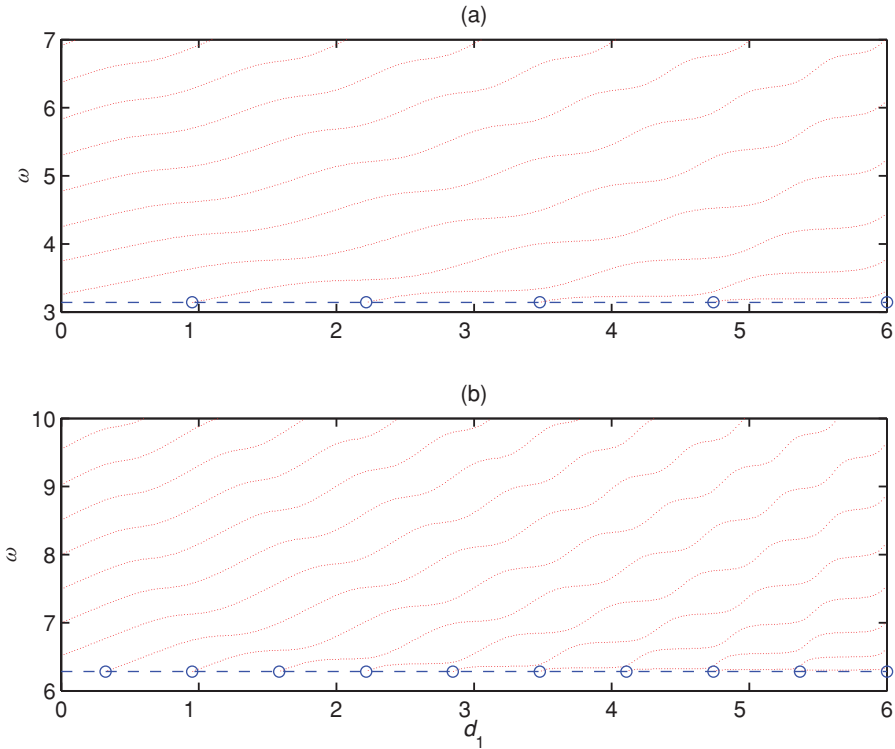


FIGURE 7. (Colour online) Surface modes for an Aluminium(1)–Tin(2) guide of constant total length $d=6$, and varying length $d^{(1)}$, for which edge $x_1=0$ is traction-free. The cut-off frequencies of material 1 are shown as dashed lines at $\omega=n\pi$, and cut-on values of $(d^{(1)}, \omega)$ are circled. (a) The $n=1$ case, and (b) the $n=2$ case.

3.5 Asymptotic analysis

Our initial idea was to find conditions on the nature of the material parameters such that one could ensure that surface waves lie solely within total stop bands of the analogous infinite structure. However, it cannot be guaranteed that such conditions exist or correspond to a material that is physically viable, and we could not obtain such conditions. Having observed the numerical results in the previous section, in particular that surface waves lie within gaps created at the edges of the Brillouin zone, it was found that one can demonstrate a partial result using asymptotic methods: that surface waves and modes of the same wavenumber across the guide (same number of half-oscillations across the guide) do not intersect. If one is able to restrict the cross sectional variation of waves in the guide to a specific mode number, n , this result coincides with our initial idea.

Definition 5 *The n -spectrum is defined to be the spectrum occupied by modes with wavenumber $n\pi/2$ across the guide. Likewise, an n -surface wave is defined to be a wave which decays in amplitude into the guide, as in (3.9), with wavenumber $n\pi/2$ across the guide. We remind the reader that n counts the number of half-oscillations of the mode, across the guide, as in (3.5).*

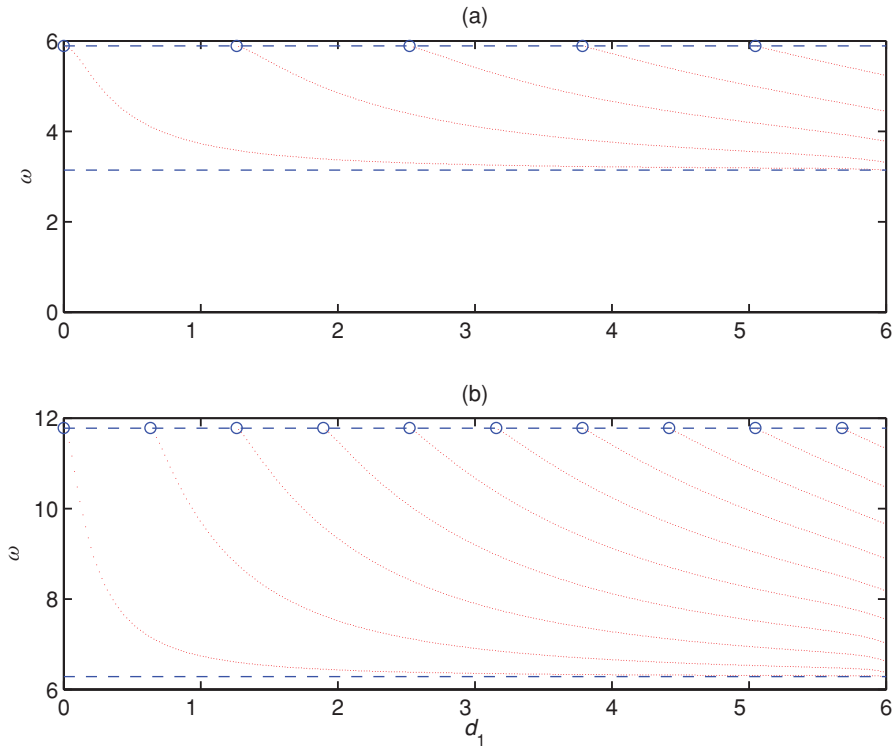


FIGURE 8. (Colour online) Surface modes for a Tin(1)–Aluminium(2) guide of constant total length $d = 6$, and varying length $d^{(1)}$, for which edge $x_1 = 0$ is traction-free. The cut-off frequencies of material 1 and 2 are shown as dashed line at $\omega = \alpha^{(1)}n\pi$ (lower) and $\omega = \alpha^{(2)}n\pi$ (upper) respectively, and cut-on values of $(d^{(1)}, \omega)$ are circled. (a) The $n = 1$ case, and (b) the $n = 2$ case.

Definition 6 An n -band gap is defined to be an interval of frequency values not occupied by the n -spectrum. For clarity, we contrast this definition against that of a total stop band, or band gap: an interval of frequency values not occupied by the Bloch spectrum. It follows that a stop band is contained within n -band gaps for all positive integer values of n , and hence no propagation is permitted.

Band gaps form even when the contrast between materials in the striped guide is weak, and we wish to exploit that fact and dissect the problem using asymptotic methods, when the edge is traction-free. In particular, we wish to demonstrate that every n -surface wave in the semi-infinite/finite problem occurs at a frequency lying within an n -band gap of the analogous infinite problem. Further such gaps of the infinite problem contain at most one such surface wave. In the straight-walled infinite case, it is readily found that frequencies bounding each band gap appear on the edge of the Brillouin zone, at $k_0d = 0, \pi$, when wall conditions are homogeneous Harrison *et al.* (2007). When the guide is homogeneous (material 1 = material 2), the case about which we will perturb, the wavenumbers along the guide at $k_0d = 0, \pi$ can be identified as $k = m\pi/d$ for $m = 0, 1, 2, \dots$ as in Adams *et al.* (2008). This result can also be demonstrated by applying (3.9) to the homogeneous case, in which $r = 1$.

A contrast between the materials is introduced by perturbing the density of material 2, setting $\rho_2 = \rho_1(1 + \epsilon)$; wave speeds are unchanged as $c_T^{(1)} = c_T^{(2)}$. We assume the ansatz $k \sim k_0 + \epsilon k_1 + \epsilon^2 k_2 + \dots$, and after noting that

$$\begin{aligned} \cos(kd^{(j)}) &\sim c_0^{(j)} - \epsilon k_0 d^{(j)} s_0^{(j)} - \epsilon^2 (k_2 d^{(j)} s_0^{(j)} + k_1^2 (d^{(j)})^2 c_0^{(j)} / 2), \\ \sin(kd^{(j)}) &\sim s_0^{(j)} + \epsilon k_1 d^{(j)} c_0^{(j)} + \epsilon^2 (k_2 d^{(j)} c_0^{(j)} - k_1^2 (d^{(j)})^2 s_0^{(j)} / 2), \\ 1/r &\sim 1 - \epsilon + \epsilon^2, \end{aligned}$$

where $c_i^{(j)} = \cos(k_i d^{(j)})$, $s_i^{(j)} = \sin(k_i d^{(j)})$, it emerges that the surface wave for the traction-free edge problem is solved by

$$k_0 = 0, \pi/d, 2\pi/d, \dots, \quad k_1 = \frac{\sin(k_0 d^{(1)}) \cos(k_0 d^{(2)})}{d \cos(k_0 d)}. \tag{3.10}$$

We now inspect the infinite case at the same frequency for which it can readily be shown that $\exp(ik_0 d) = [\text{tr}(\mathcal{M}) \pm \sqrt{\text{tr}(\mathcal{M})^2 - 4}] / 2$, where $\text{tr}(\cdot)$ denotes the matrix trace and \mathcal{M} is given in (3.7). Hence $|\text{tr}(\mathcal{M})| > 2$ whenever a band gap is present, Adams et al. (2008). This result also holds for fixed n : $|\text{tr}(\mathcal{M}_n)| > 2$ whenever an n -band gap is present; we append the subscript n to \mathcal{M} to emphasise that this is \mathcal{M} for the n th mode. We wish now to exploit that fact to demonstrate that the value of k given in (3.10) always lies within a band gap of the infinite problem.

The trace of \mathcal{M}_n given by (3.7), simplifies to

$$\text{tr}(\mathcal{M}_n) = 2\mathcal{C}^{(1)}\mathcal{C}^{(2)} - (r + r^{-1})\mathcal{S}^{(1)}\mathcal{S}^{(2)},$$

which, by applying the aforementioned expansions, takes the form

$$\text{tr}(\mathcal{M}_n) \sim 2 \cos(k_0 d) - \epsilon^2 [k_1^2 d^2 \cos(k_0 d) + \sin(k_0 d^{(1)}) \sin(k_0 d^{(2)})].$$

Noting that $|2 \cos(k_0 d)| = 2$, the sign of the first non-zero correction term will determine whether or not the surface mode lies in a band gap. The omission of an $\mathcal{O}(\epsilon)$ term physically corresponds to the fact that the sign of the density perturbation does not affect this.

Evaluating this at the wavenumber of the surface wave, found in (3.10), we arrive at:

$$\text{tr}(\mathcal{M}_n) \sim 2 \cos(k_0 d) \left(1 - \frac{\epsilon^2 T}{\cos^2(k_0 d)} \right),$$

where

$$T = \cos^2(k_0 d^{(2)}) \sin^2(k_0 d^{(1)}) + \sin(k_0 d^{(1)}) \sin(k_0 d^{(2)}) \cos(k_0 d).$$

By noting that $\sin(k_0 d^{(2)}) = -\cos(k_0 d) \sin(k_0 d^{(1)})$, it is quickly shown that

$$T = \sin^2(k_0 d^{(1)}) (\cos^2(k_0 d^{(2)}) - 1) \leq 0,$$

and equality is only achieved if $k_0 d^{(1)} = m\pi$. It thus follows that away from these values, which we return to later, $\text{tr}(\mathcal{M}_n) > 2$, and thus the n -surface wave lies outside of the n -spectrum. For given parameters, (3.10) has a unique solution k_1 , and this also holds true for higher-order terms. As each surface wave is perturbed off a different frequency,

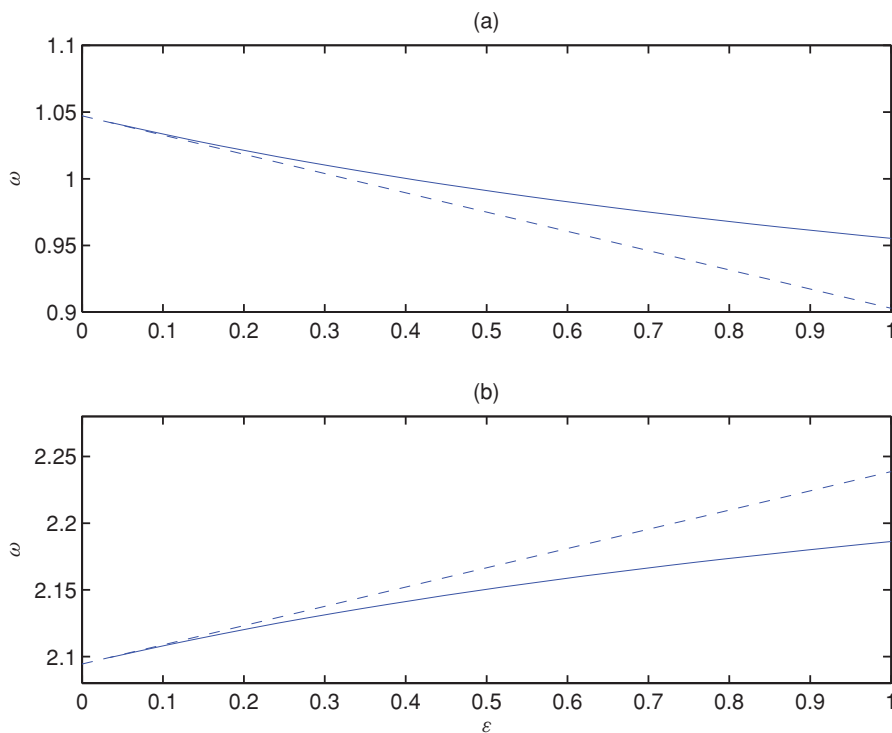


FIGURE 9. (Colour online) Dashed curves show the surface wave solutions from the asymptotic scheme, found using (3.10). Solid curves show the computational solution, found by root finding on equation (3.9). (a), (b) The first two modes respectively.

each n -band gap in the spectrum can have at most one surface wave in it. In fact we find numerically exactly one surface wave in each gap. It is worth noting that in the clamped case (not shown), for which the $n = 0$ mode is excluded, that the lowest gaps for $n = 1$ had no surface wave within them.

Having developed an asymptotic scheme, we now compare it to the numerical solution of (3.9), as ϵ increases. Figure 9 shows the lowest two modes, perturbed off $\omega = \pi/d, 2\pi/d$, and we consider a case with $d^{(1)} = 4$, $d^{(2)} = 2$. The agreement is good up to $\epsilon = 1$, with a relative error of 5.5% for the first mode and 2.4% in the second. We attribute the exceptional accuracy of this scheme at high ϵ to the increasingly many sin, cos terms multiplying higher-order corrections. Having established that the asymptotic scheme developed produces results close to those found from the full computation, we can be confident in the findings that scheme led to; namely the demonstration that at a fixed wavenumber, $n\pi/2$, the infinite spectrum and surface waves do not intersect.

4 Concluding remarks

Here we have considered a ‘1.5-dimensional’ waveguide problem which is intermediate between that of a simple line and of a fully two-dimensional composite structure. We are interested in how the spectrum of the guide, with unit length, is affected as the guide height, η , tends to 0. In particular, we address the problem when the wavelength across

the guide remains of the order of magnitude of the guide height as $\eta \rightarrow 0$. The limit spectrum, $\sigma_{\text{Bloch}} \cup \sigma_{\text{boundary}}$, consists of two parts: the Bloch spectrum, which is readily found as in Adams *et al.* (2008), and the unknown boundary spectrum, about which one cannot say *a priori* whether it is non-empty, and, in particular, whether $\sigma_{\text{boundary}} \setminus \sigma_{\text{Bloch}}$ is non-empty. The limit spectrum was shown to coincide with the spectrum σ_{Π} of a problem on $\Pi = \mathbb{R}_+ \times (-1/2, 1/2)$. Hence, if we know that the spectrum σ_{Π} has a point part (i.e. eigenvalues) away from σ_{Bloch} , then these eigenvalues must be elements of the boundary spectrum σ_{boundary} .

This analysis was complemented by numerical work, in which we considered the problem on Π . Material parameters were set to vary in a piecewise periodic fashion so the analogous guide of infinite length coincides with the striped guide considered in Adams *et al.* (2008), allowing the Bloch spectrum to be readily obtained. The aim was to demonstrate numerically that σ_{boundary} is non-empty by invoking (2.26) and by comparing this spectrum σ_{Π} to σ_{Bloch} . To this end, we restricted ourselves to those solutions that exponentially decay into the guide and satisfy an additional restriction that allows us to study an equivalent problem on a single period cell. Using this observation we can capture some, but not necessarily all, of the elements in σ_{boundary} ; this spectrum may indeed be far richer than a collection of discrete points found using the methodology contained herein. One could for instance use the alternative approach of Movchan & Slepyan (2007) whereby localised modes are sought in the form of (anisotropic) Greens functions in the gaps, and this may pick up other types of boundary modes.

We have provided a methodology to find such surface waves in finite and semi-infinite straight walled striped guides with homogeneous conditions on the walls using a modal matrix approach. Surface mode shapes and frequencies were given and a discussion of the length scale over which the mode decays was presented. Investigation into a problem with layers of infinite height, in which no restrictions are placed on wavenumber across the guide, offered further insight into the guide problem. Results of surface waves and analogous infinite guides were presented, and observations made about the frequency of the surface modes relative to band gaps of the analogous infinite structure. In particular, we observed that all surface modes exist within gaps of the infinite spectrum with the same wavenumber, even when those band gaps are narrow. We later used this observation as the basis for an asymptotic scheme, developed with a view to demonstrating this relationship in the special case of weak material contrast. In this situation, it was found surface modes lie within gaps in the spectrum when the wavenumber across the guide is held constant: to use the terminology developed herein, n -surface waves always lie in n -band gaps. Notably this implies that at sufficiently low frequencies, below the cut-on for $n = 1$ modes, surface modes lie in total stop bands of the infinite problem. This asymptotic scheme was compared against numerical results, and its accuracy demonstrated.

References

- ADAMS, S. D. M., CRASTER, R. V. & GUENNEAU, S. (2008) Bloch waves in multi-layered acoustic waveguides. *Proc. R. Soc. Lond. A* **464**, 2669–2692.
- ADAMS, S. D. M., CRASTER, R. V. & GUENNEAU, S. (2009) Guided and standing Bloch waves in periodic elastic strips. *Waves RandomComplex Media* **19**, 321–346.

- ALLAIRE, G. (1992) Homogenization and two-scale convergence. *SIAM J. Math. Anal.* **23**(6), 1482–1518.
- ALLAIRE, G. & CAPDEBOSCO, Y. (2002a) Homogenization and localization for a 1-D eigenvalue problem in a periodic medium with an interface. *Ann. Mat. Pura Appl. (4)* **181**, 247–282.
- ALLAIRE, G. & CAPDEBOSCO, Y. (2002b) Homogenization and localization for a 1-D eigenvalue problem in a periodic medium with an interface. *Ann. Mat.* **181**, 247–282.
- ALLAIRE, G. & CONCA, C. (1996) Bloch wave homogenization for a spectral problem in fluid-solid structures. *Arch. Ration. Mech. Anal.* **35**(3), 197–257.
- ALLAIRE, G. & CONCA, C. (1998) Boundary layers in the homogenization of a spectral problem in fluid-solid structures. *SIAM J. Math. Anal.* **29**, 343–379.
- ALLAIRE, G. & CONCA, C. (1998b) Bloch wave homogenization and spectral asymptotic analysis. *J. Math. Pures. Appl.* **77**, 153–208.
- BENSOUSSAN, A., LIONS, J. L. & PAPANICOLAOU, G. (1978) *Asymptotic Analysis for Periodic Structures*, North-Holland, Amsterdam.
- CAMLEY, R. E., DJAFARI-ROUHANI, B., DOBRZYNSKI, L. & MARADUDIN, A. A. (1983) Transverse elastic waves in periodically layered infinite and semi-infinite media. *Phys. Rev. B* **27**(12), 7318–7329.
- CASTRO, C. & ZUAZUA, E. (1996) Une remarque sur l'analyse asymptotique spectrale en homogénéisation. *C. R. Acad. Sci. Paris Sér. I Math.* **322**, 1043–1047.
- CASTRO, C. & ZUAZUA, E. (2000a) Low frequency asymptotic analysis of a string with rapidly oscillating density. *SIAM J. Appl. Math.* **60**(4), 1205–1223.
- CASTRO, C. & ZUAZUA, E. (2000b) High Frequency asymptotic analysis of a string with rapidly oscillating density. *Euro. J. Appl. Math.* **11**(6), 595–622.
- CHEREDNICHENKO, K. D. & GUENNEAU, S. (2007) Bloch wave homogenisation for spectral asymptotic analysis of the periodic Maxwell operator. *Waves Random Complex Media* **17**, 627–651.
- CONCA, C., PLANCHARD, J. & VANNINATHAN, M. (1995) *Fluids and Periodic Structures*, RMA, J. Wiley and Masson, Paris.
- DOSSOU, K. B., MCPHEDRAN, R. C., BOTTEN, L. C., ASATRYAN, A. A. & DE STERKE, C. M. (2007) Gap-edge asymptotics of defect modes in 2D photonic crystals. *Opt. Express* **15**, 4753–4762.
- FIGOTIN, A. & KUCHMENT, P. (1996) Band-gap structure of the spectrum of periodic and acoustic media. Part I. Scalar model. *SIAM J. Appl. Math.* **56**, 68–88.
- FIGOTIN, A. & VITEBSKIY, I. (2006) Slow light in photonic crystals. *Waves Random Complex Media* **16**, 293–382.
- GRALAK, B., ENOCH, S. & TAYEB, G. (2000) Anomalous refractive properties of photonic crystals. *J. Opt. Soc. Am. A* **17**, 122–131.
- HARRISON, J. M., KUCHMENT, P., SOBOLEV, A. & WINN, B. (2007) On occurrence of spectral edges for periodic operators inside the Brillouin zone. *J. Phys. A – Math.* **40**, 7597–7618.
- KOHN, W. & LUTTINGER, J. (1955) Theory of donor states in silicon. *Phys. Rev.* **98**, 915–922.
- KRONIG, R. L. & PENNEY, W. G. (1931) Quantum mechanics in crystal lattices. *Proc. R. Soc. A* **130**, 499–531.
- KUCHMENT, P. (1993) *Floquet Theory for Partial Differential Equation*, Birkhäuser, Basel.
- LIN, S. Y., HIETALA, V. M., WANG, L. & JONES, E. D. (1996) Highly dispersive photonic band gap prism. *Opt. Lett.* **21**, 1771–1773.
- LOBO, M. & PÉREZ, E. (2001) The skin effect in vibrating systems with many concentrated masses. *Math. Meth. Appl. Sci.* **24**, 59–80.
- MOVCHAN, A. B. & SLEPYAN, L. I. (2007) Band gap Greens functions and localized oscillations. *Proc. R. Soc. Lond. A* **463**, 2709–2727.
- NGUETSENG, G. (1989) A general convergence result for a functional related to the theory of homogenization. *SIAM J. Math. Anal.* **20**, 608–623.
- PENDRY, J. B. (1994) Photonic band structures. *J. Mod. Opt.* **41**, 209–229.
- POULTON, C. G., BOTTEN, L. C., MCPHEDRAN, R. C., NICOROVICI, N. A. & MOVCHAN, A. B. (2001) Noncommuting limits in electromagnetic scattering: asymptotic analysis for an array of highly conducting inclusions. *SIAM J. Appl. Math.* **61**, 1706–1730.

- PAGNEUX, V. & MAUREL, A. (2002) Lamb wave propagation in inhomogeneous elastic waveguides. *Proc. R. Soc. Lond. A* **458**, 1913–1930
- RUSSELL, P. S., MARIN, E., DIEZ, A. GUENNEAU, S. & MOVCHAN, A. B. (2003) Sonic band gap PCF preforms: Enhancing the interaction of sound and light. *Opt. Express* **11**, 2555.
- ZHIKOV, V. V. (2000) On an extension of the method of two-scale convergence and its applications. *Sb. Math.* **191**(7–8), 973–1014.
- ZOLLA, F., BOUCHITTE, G. & GUENNEAU, S. (2008) Pure currents in foliated waveguides. *Q. J. Mech. Appl. Math.* **61**(6), 453–474.